Article

Health Risks Forecast of Regional Air Pollution on Allergic Rhinitis: High-Resolution City-Scale Simulations in Changchun, China

Weifang Tong [1], Xuelei Zhang [2,*], Feinan He [1], Xue Chen [2], Siqi Ma [3], Qingqing Tong [2], Zeyi Wen [2,4] and Bo Teng [1,*]

[1] Department of Otolaryngology Head and Neck Surgery, The Second Hospital, Jilin University, Changchun 130041, China
[2] Key Laboratory of Wetland Ecology and Environment, Northeast Institute of Geography and Agroecology, Chinese Academy of Sciences, Changchun 130102, China
[3] Department of Atmospheric, Oceanic and Earth Sciences, George Mason University, Fairfax, VA 22030, USA
[4] University of Chinese Academy of Sciences, Beijing 100049, China
[*] Correspondence: zhangxuelei@neigae.ac.cn (X.Z.); tengbo@jlu.edu.cn (B.T.)

Abstract: Accurate assessments of exposure to urban air pollution with higher traffic emissions and its health risks still face several challenges, such as intensive computation of air pollution modeling and the limited availability of personal activity data. The macroscopic health effects can be transmitted to the whole population for personal prevention via air quality health index (AQHI), but the possibility risk index of the specific allergic diseases is still lacking. This interdisciplinary study aims at evaluating the forecasted results of high-resolution air quality with updated traffic emissions and accessing the potential impacts of outdoor pollution on morbidity of rhinitis for urban residents. A high-resolution modelling system (1 km × 1 km) containing the online traffic emission model (VEIN), meteorological and air quality model (WRF-CHIMERE) and the health impact module was developed. A new health index of Potential Morbidity Risk Index (PMRI) was further established using higher resolution health risk coefficients of major air pollutants on allergic rhinitis, and different methods (with/without considering population distributions) targeting different user groups (residents, hospitals and health administrations) were calculated and analyzed. Operational forecasted results of hourly PMRI can be further combined with online map services to serve as an effective tool for patients with allergic rhinitis to arrange their daily activities so as to avoid acute exacerbation. The forecasted PMRIs accessible to the public will also be beneficial for the public health administrations in planning the medical resource and improving the outpatient efficiency.

Keywords: allergic rhinitis; air quality forecast; relative risks; potential morbidity risk index; personal prevention

1. Introduction

Rapid urbanization and economic growth have given rise to severe air pollution in urban areas in developing countries. The ambient air pollution can result in serious human health effects and has aroused wide concern of the public, media and even the government [1,2]. Exposure to either gaseous or particulate matters can increase morbidity or/and mortality of various diseases, such as non-accidental death, respiratory, cardiovascular, cardiopulmonary diseases and so on [3,4]. The health effects of different components together with their emission sources in the atmospheric environment have also been widely reviewed, such as desert dust [5], black carbon [6–8], elemental carbon [9], biomass smoke and traffic emissions [10–13].

Over the past decade, there has been a need to quantitatively estimate the effects of outdoor air pollution on human health, which has facilitated the development of interdisciplinary

research among epidemiology, atmospheric modeling and remote sensing. The 3D air quality models based on Eulerian dispersion methods running at different scales have been applied in quantitative estimation of health impacts, such as GEOS-Chem and LMDz-INCA simulations at global-scale [14–17], the CMAQ [18–21], WRF-Chem [22–24], CAMx [25–30] and CHIMERE [31–33] simulations at regional/country-scale, and the ADMS-Urban simulations at street-scale [34]. Air quality models are usually adopted to provide the historical or/and spatially interpolated data of pollutant concentrations in epidemiological studies, and even output the Air Quality Health Index (AQHI) to the public for personal prevention. Among these studies, researchers mainly paid attention to investigating the health impacts of $PM_{2.5}$/gaseous pollutants from specific emission sources, such as power plants [35–37] and oil and natural gas sector emissions [38], and focused more on the sensitivity of using different grid resolutions in simulations to the estimated health assessment results [39–41]. Thompson et al. [25] demonstrated that the estimated health benefits calculated with coarse resolution (36 km × 36 km) would be twice greater than finer scale results (4 km × 4 km) in urban areas, and some regions even showed decreasing estimated health effects as grid resolution increased. It suggested that numerical simulations of air quality in higher spatial resolutions are more necessary for accurately assessing the health risks/benefits for personal exposures in urban areas. Recently, a few studies have set the highest spatial resolutions of 1 km at city scale to provide insight into the health effects of exposure to ambient pollution [42].

Previous interdisciplinary studies focus mainly and retrospectively on the estimations of health risks of long-term exposure to ambient pollution or prospectively on the health benefits under the implementation of air pollution control policies. There are only limited studies focusing on the quantitative calculation of acute respiratory diseases caused by short-term exposure to outdoor air pollution, such as allergic rhinitis and acute exacerbation of asthma. Allergic rhinitis (AR) affects 20–40% of the population worldwide and presents with symptoms that affect quality of life and work productivity, although the morbidity varies with age and region [43–45]. Asthma is a complex heterogeneous and chronic inflammatory disease with an increasing morbidity worldwide. About 1.85 million new pediatric asthma cases are attributable to NO_2 globally in 2019, two-thirds of which occur in urban areas [46]. Asthma is categorized as primary or secondary. The former means the risk of new asthma/allergic rhinitis occurrence and the latter relates to triggering the acute exacerbation of allergic diseases [47].

Previous time-series, cross-sectional and cohort studies have demonstrated the positive associations between vehicle emissions and increased risk of asthma and AR [48–53]. Individual pollutants responsible for the increased risk of AR are $PM_{2.5}$, PM_{10}, NO_2, SO_2 and O_3, except for CO [45,54–56]. Five years have passed since the publication of Teng et al. [43], but the association between local ozone pollution and morbidity of AR in China is still unclear. For asthma, the review and meta-analysis studies have consistently showed that the air quality components positively associated with the acute asthma exacerbation are NO_2, $PM_{2.5}$, PM_{10}, O_3, Benzene and TVOCs [57–61], and SO_2 is not significantly associated with the morbidity of asthma during short-term exposure in East Asia [62,63]. However, the latest study of Kindzierski et al. [64] has evaluated the reliability of observational base studies that are used in the meta-analysis research of Zheng et al. [59] via *p*-value plots, and has suggested that the meta-analysis of acute asthma exacerbation with exposure to six air pollutants is unreliable and false-positives due to the presence of multiple testing and multiple modelling bias in the based epidemiological papers. The reliability of other meta-analysis studies also needs to be further examined. The main research gap remains, namely, that the macroscopic health effects can be transmitted to the whole population through AQHI for personal prevention, but the possibility risk index of the specific allergic diseases is still lacking.

Besides the air pollutants, meteorological factors also have important influence on the occurrences of AR, especially for the temperature changes [65,66] and relative humidity [67,68]. Initially, the effects of increased temperature on AR were less concerned in

China [69]. Teng et al. [43] was the first group that comprehensively analyzed the exposure–response relationships between all the meteorological factors and outpatients of allergic rhinitis, and revealed that the lower temperatures (<0 °C) and lower relative humidity (<58%) were significantly associated with higher AR risks. Duan et al. [68] reported that outpatients attributable to lower values (33%–64%) of RH were 5.22% (95% CI: 1.92%, 8.33%) and higher values of RH (>76%) were 4.07% (95% CI: 1.13%, 7.30%) with 4-days lagged effects in Hefei, China. In the same city, the lower temperatures (−12.2–5.9 °C) during nighttime were significantly associated with increased risk of AR, and a 3.8 °C decrease at night could lead to an increase of 2% (95% CI: 1–4%) in the daily outpatient admissions for all children with AR [70]. Daily mean temperature and atmospheric pressure were significantly associated with −7.6% and 7.5% increasing of allergic diseases in children in Shanghai [55]. The negative association was also reported for all population in Xinxiang of central China [71]. The effects of $PM_{2.5}$, PM_{10} and NO_2 on AR outpatients were enhanced at lower temperatures (−14.3–2.8 °C) and higher humidity (>67%) in Beijing [72]. An M-shaped relationship between ambient temperature and allergic rhinitis outpatient in Xinxiang of central China was reported by J. Gao et al. [73] and the higher risk peak located at lower temperatures of 1.6–9.3 °C (another peak presented in 23.5–28.5 °C, which overlapped with the allergic effects of pollens).The temperature was determined as negatively related to the AR occurrence in Taiwan, and each increasing of 10% in RH and 1 °C in temperature was related to 9.2% and 1.2% reduction in AR occurrence, respectively [74]. Moreover, Kim et al. [75] further discovered that the cold temperatures (−1.7–7.9 °C) had significant effect on increasing hospital visits by allergic rhinitis in the total population especially for the elders in Seoul, South Korea, and a significant increase in AR cases with lower relative humidity in Busan was also observed [67].

As mentioned above, it is also necessary to account for the specific short-term health effects of lower temperatures on the occurrence of allergic rhinitis at the city scale, and the localized coefficient of exposure risk should be gained via time-series analysis before conducting the forecast calculation of the potential morbidity risks. Based on our previous basis of local time-series research [43], our current study focuses solely on the allergic rhinitis (the methodology of this study is also applicable to other allergic diseases, such as asthma and allergic conjunctivitis) and aims to develop a numerical forecast system (built on the cloud computing platform) that can evaluate the potential morbidity risk of acute allergic diseases (such as AR) for short-term (hourly and daily) exposure to outdoor traffic pollution at city scale (1 km × 1 km) for the next 24 h, and can automatically generate scientific protection advice for the public and local health administrations.

2. Methodology

2.1. Domain Setting

Hourly forecasted pollutants (CO, NO_2, O_3, $PM_{2.5}$ and PM_{10}) concentrations in Changchun in July and December of 2021 have been simulated at the high horizontal grid resolution (1 km × 1 km) using the air quality model of CHIMERE v2017r4. The model grid domain of WRF-VEIN-CHIMERE forecast system covers the entire downtown area of Changchun and parts of other 6 adjacent counties as illustrated in Figure 1. The road networks obtained from OpenStreetMaps are also presented in Figure 1.
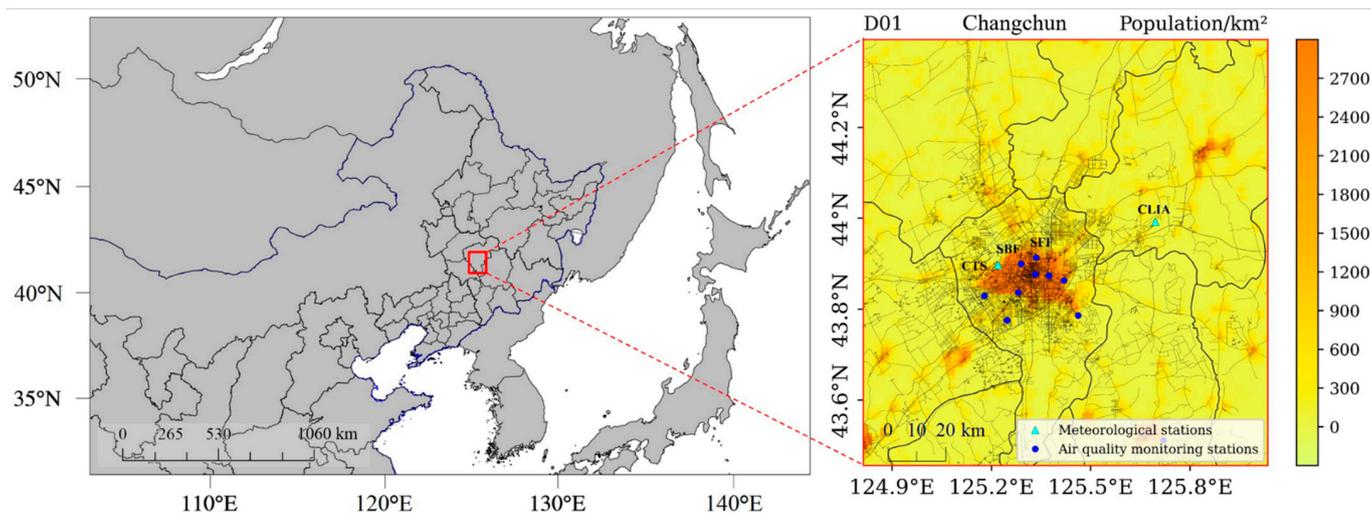
Figure 1. Model domain setting of WRF-VEIN-CHIMERE system and spatial distribution of population, road networks and observation sites in Changchun, Northeast China.

2.2. Data Sources

The health effects of different ambient pollutants on asthma and AR were collected through Google scholar, PubMed, Web of Science and Scopus and then Meta-analyzed to obtain the median values with uncertainties.

The ground-based hourly observation data of $PM_{2.5}$, PM_{10}, O_3, CO and NO_2 concentrations between the two simulation periods were obtained from the Changchun Municipal Environmental Protection Monitoring Center. The meteorological parameters of hourly temperatures, humidity and wind velocity used for validation of simulation results were downloaded from the Weather Underground website (www.wunderground.com, accessed on 12 February 2023).

2.3. Model Configurations and Optimizations

The air quality model of CHIMERE was adopted to produce hourly forecasted air quality data in this study. CHIMERE is a multi-scale Eulerian chemistry-transport model (CTM) which is commonly used in simulating/forecasting hourly concentrations of aerosol and gaseous pollutants with horizontal resolution ranging from city to global scales [76]. The Weather Research and Forecasting (WRF) model version 3.9.1 was used to generate the meteorological output fields to drive the running of CHIMERE model. All the modeling system configuration details are concisely summarized in Table 1. As the Global Forecast System forecast products of the National Center for Environmental Prediction (GFS-NCEP) were frequently used as a meteorological input during the numerical forecast, data with a horizontal resolution of $0.5° \times 0.5°$ (available every 6 h) were introduced to act as the initial and boundary fields for the WRF model in this study (https://www.ncdc.noaa.gov/data-access/model-data/model-datasets/global-forcast-system-gfs, accessed on 12 February 2023).

As listed in Table 1, the chemistry mechanism of MELCHIOR2 in the CHIMERE model (version 2017r4) was enabled. The Multi-resolution Emission Inventory for China (MEIC) without considering the emission data of the transportation sector for the year 2017 was introduced as the anthropogenic emissions and pre-processed by a modified version of emiSURF program (version 2016b) before being incorporated into the model domain. The outermost boundaries of the meteorological driving field were removed, and there were 96×102 grid points in the domain of CHIMERE. The vertical levels of the model were increased from 8 (surface to 500 hPa) to 15 (surface to 200 hPa) to obtain more detailed vertical results. All the hindcast simulations were run for the future 48 h from 24 June to 31 July and 24 November to 31 December 2021, and the simulated results of first 7 days were treated as spin-up period and discarded in the following data analysis processes.

Table 1. Model configurations of WRF-VEIN-CHIMERE forecast system.

Models	Parameters	Configurations
WRF	Projection	Lambert
	Number of domain	1
	Vertical layers	30
	Horizonal resolution	1 km × 1 km
	Grids	99 × 105
	Time step	60 s
	Microphysics scheme	Milbrandt–Yau Double Moment Scheme
	Short wave and Longwave Radiation	RRTMG Scheme
	Planetary boundary layer	Asymmetric Convection Model 2 Scheme
	Land-surface	Pleim–Xiu Land Surface Model
	Cumulus option	Grell 3D Ensemble Scheme
CHIMERE	Chemistry scheme	MELCHIOR2
	Gas and aerosol partition	ISORROPIA
	Horizontal advection	Van Leer
	Vertical advection	Van Leer
	Dry deposition	Zhang_2001
	Initial conditions	Previous forecast result
	Boundary conditions	LMDz-INCA + GOCART
	Dust emissions	GOCART
	Biogenic emissions	MEGAN V3
	Anthropogenic emissions	MEIC_2017
	Traffic emissions	VEIN_2020

The high-resolution vehicular emissions inventory for Northeast China which was compiled by the open-source Vehicular Emissions Inventory model (VEIN) [77,78] was used in this study. This inventory included 133 pollutants from the 36 municipalities of Northeast China and it has recently updated to the base year of 2020. The traffic emission was further merged with preprocessed anthropogenic emission including the temporal allocation and chemical species mapping via R programming language (Version 4.1.0).

In order to improve the model performance at the city/street scale, besides compiling a new high-resolution traffic emissions inventory, the model optimizations mainly include changing the WRF to WRF-Urban model to account for the urban building canopy effects and enabling a corresponding simple urban canopy correction option in CHIMERE to enhance the forecast accuracy for diffusion conditions in the first urban layer (the correction coefficient of Kz is set to 0.45).

2.4. Selection of Health Effect Estimates for Allergic Rhinitis

The epidemiological studies referring to health effects of exposing to air pollution can be sorted into two categories: the time-serious studies and the cross-sectional studies [79]. All the AR related studies conducted in China were summarized in Table 2, and can be sorted into three groups: 18 cross-sectional studies using multi-variables/multi-levels logistic regression models, 5 cohort studies and 8 time-serious studies to fix the health risks of AR during acute exposure.

The quantitative health effects are always reported as risk ratios (RRs), odds ratios (ORs) and/or hazard ratios (HRs) [80]. Risk ratios (or named as Relative Risks) and odds ratios are common but easily misused/misunderstood statistical measures in epidemiological cross-sectional studies. ORs may overestimate the relative risks of a disease when the prevalence is high [81], such as the AR in this study. Only when a disease is exceedingly rare within a population can the ORs be considered as equivalent to RRs [80,82]. It should be noted that OR is a relative measure just as RR, and thus sometimes a large OR can correspond with a small difference between odds. In most reports, then, OR should not

be presented as an RR, and should only be presented as an approximation of RR in rare diseases. If possible, an RR should always be reported.

Table 2. Summary of collected epidemiological studies referring to allergic rhinitis and air quality in 2005–2022.

Case Studies					Meta-Analysis Studies				
Reference	Study Areas	Study Design	Indices	Methods *	Zou et al., 2018 [54]	Lin et al., 2021 [83]	Zhang et al., 2022 [84]	Li et al., 2022 [45]	Jia et al., 2022 [56]
Hwang et al., 2006 [85]	Taiwan	Cross-sectional	ORs	LRM		✓		✓	
Dong et al., 2011 [86]	7 cities of Northeast China	Cross-sectional	ORs	LRM		✓		✓	
Lu et al., 2013 [87]	Changsha	Cross-sectional	ORs	LRM	✓	✓	✓	✓	
Liu et al., 2013 [88]	7 cities of Northeast China	Cross-sectional	ORs	LRM	✓	✓	✓	✓	
Deng et al., 2016 [49]	Changsha	Cohort	ORs	LRM	✓	✓	✓	✓	
Liu et al., 2016 [89]	Shanghai	Cohort	ORs	LRM	✓	✓	✓	✓	
Wang I. et al., 2016 [90]	Taipei	Cohort	ORs	LRM	✓	✓	✓	✓	
Chung et al., 2016 [91]	Taiwan	Cohort	ORs	LRM	✓	✓	✓	✓	
Li et al., 2019 [92]	Taiwan	Cohort	HRs	LRM					✓
Chen et al., 2016 [93]	Taiwan	Case-crossover	ORs	LRM					
Chen et al., 2018 [94]	6 cities of China	Cross-sectional	ORs	LRM	✓	✓	✓	✓	✓
Norbäck et al., 2018 [95]	6 cities of China	Cross-sectional	ORs	LRM	✓	✓	✓		
Huang et al., 2019 [96]	Wuhan &Ezhou	Cross-sectional	ORs	LRM		✓	✓	✓	
Liu et al., 2020 [97]	Shanghai	Cross-sectional	ORs	LRM			✓	✓	
Hao et al., 2021 [53]	Shenyang	Case-control	ORs	LRM			✓		
Hsieh et al., 2020 [74]	Taiwan	Cross-sectional	ORs	LRM				✓	
Wang et al., 2021 [98]	China	Cross-sectional	ORs	LRM				✓	
Chen et al., 2019 [99]	Jinan	Time-series	ORs	LRM					✓
Zhang et al., 2011 [100]	Beijing	Time-series	RRs	GAM					
Zhang et al., 2016 [101]	Beijing	Time-series	RRs	GAM					✓
Teng et al., 2017 [43]	Changchun	Time-series	RRs	GAM					✓
Chu et al., 2019 [102]	Nanjing	Time-series	RRs	GAM					✓
Wang et al., 2019 [103]	Beijing	Time-series	RRs	GAM					✓
Wang et al., 2019 [71]	Xinjiang	Time-series	RRs	GAM					✓

Table 2. *Cont.*

	Case Studies				Meta-Analysis Studies				
Reference	Study Areas	Study Design	Indices	Methods *	Zou et al., 2018 [54]	Lin et al., 2021 [83]	Zhang et al., 2022 [84]	Li et al., 2022 [45]	Jia et al., 2022 [56]
Wu et al., 2022 [72]	Beijing	Time-series	RRs	GAM					
Guo et al., 2022 [104]	Wuhan	Time-series	RRs	GAM					
Luo et al., 2022 [105]	Guangzhou-Shenzhen-Zhuhai	Time-series	RRs	GAM					

* LRM: logistic regression model; GAM: Generalized additive model; $\sqrt{}$ means this study is collected and included in the corresponding meta-analysis studies.

As shown in Table 2, 17 studies reported the results of ORs, 8 studies presented the RRs and only 1 study reported the HRs. In recently published meta-analysis studies, 4 out of 5 focused on the reported ORs, which means that these studies may overestimate the RRs of AR as the prevalence is only as high as 8.7–24.1% of population in China (Figure 1 in Reference [43]). The time series analysis is more apt to forecast a future condition, and the cross-sectional analysis is better to find out the near-term future of the potential prevalence of a disease. Moreover, for the works related to health care planning, the RRs should be adopted in the studies as advised in Andrade [106]. Recently, Slama et al. [107] have demonstrated that both case-crossover and time-series analysis methods provide the consistent trends and the overlap of the results for air pollution effects on short-term hospitalizations of respiratory diseases in Poland. However, our compiled result revealed contradicting result that the health effects reported from the cross-sectional studies were 5–20 times larger than time-series studies for AR in China (Table 3). Thus, to be more stringent, the reported RRs for each positive correlated pollutants from the city of Changchun in Teng et al. [43] and the averaged values of RRs among 6 time-series analysis studies (in Tables 2 and 3) were further used in the calculation of potential morbidity risks when acute exposure to the local forecasted air pollution.

Table 3. The compiled relative risks of exposure to various ambient pollutants with a 10 $\mu g/m^3$ increase in single case studies and meta-analysis studies.

Reference	Published Year	Age Groups	Study Areas	PM$_{2.5}$	PM$_{10}$	NO$_2$	O$_3$	CO *	SO$_2$
Zou et al., 2018 [54]	2018	Children	Meta-analysis	1.163 (1.074–1.260)	1.075 (0.995–1.161)	1.236 (1.099–1.390)			1.044 (0.954–1.142)
Zhang et al., 2022 [84]	2021	Children	Meta-analysis	1.15 (1.03–1.29)	1.02 (1.01–1.03)	1.11 (1.05–1.18)	**0.98 (0.67–1.41)**		1.03 (1.01–1.05)
Lin et al., 2021 [83]	2021	Children	Meta-analysis	1.09 (1.01–1.17)	1.06 (1.02–1.11)				
Jia et al., 2022 [56]	2022	Children	Meta-analysis	1.08 (1.04–1.13)					
Li et al., 2022 [45]	2022	All_ages	Meta-analysis	1.12 (1.05–1.20)	1.13 (1.04–1.22)	1.13 (1.07–1.20)	1.07 (1.01–1.12)	1.07 (0.99–1.17)	1.13 (1.04–1.22)
Jia et al., 2022 [56]	2022	All_ages	Meta-analysis	1.21 (1.01–1.44)					
Zhang et al., 2011 [100]	2011	All_ages	Beijing			1.0073 (1.0066–1.0080)	1.0512 (1.0483–1.0542)		1.0010 (1.0005–1.0014)
Chen et al., 2016 [93]	2016	All_ages	Taibei		1.067 (1.055–1.080)	1.130 (1.115–1.145)	1.118 (1.100–1.136)	1.148 (1.125–1.170)	**0.990 (0.975–1.005)**
Teng et al., 2017 [43]	2017	All_ages	Changchun	1.102 (1.055–1.151)	1.049 (1.008–1.092)	1.111 (1.058–1.165)	**0.993 (0.941–1.048)**	**0.977 (0.907–1.053)**	1.002 (0.985–1.015)
Wang et al., 2016 [90]	2016	Children	Taibei	1.54 (1.03–2.32)	1.15 (0.79–1.45)	0.95 (0.79–1.66)	1.01 (0.76–1.34)	1.02 (0.8–1.29)	1.00 (0.78–1.29)
Chung et al., 2016 [91]	2016	Children	Taiwan			1.12 (0.79–1.45)	1.27 (0.76–1.70)	1.14 (1.02–1.86)	1.05 (0.67–1.22)
Chu et al., 2019 [102]	2019	All_ages	Nanjing	1.0539 (1.0273–1.0812)	1.0586 (1.0300–1.0881)				1.085 (0.982–1.198)
Wang et al., 2020 [103]	2020	All_ages	Beijing	1.0047 (1.0039–1.0055)					
Wang et al., 2020 [71]	2020	All_ages	Xinjiang	1.007 (1.000–1.0141)		1.0079 (1.0035–1.0123)	1.0454 (1.0301–1.0608)	1.0097 (0.9989–1.0205)	1.0007 (1.0002–1.0012)
Wu et al.,2022 [72]	2022	All_ages	Beijing	1.0124 (1.0069–1.0178)	1.0079 (1.0043–1.0115)	1.0305 (1.0172–1.0440)		1.0501 (1.0118–1.0896)	1.0343 (1.0147–1.0539)

Table 3. *Cont.*

Reference	Published Year	Age Groups	Study Areas	PM$_{2.5}$	PM$_{10}$	NO$_2$	O$_3$	CO *	SO$_2$
Li S. et al., 2022 [108]	2022	All_ages	Beijing	1.010 (0.985–1.035)	1.012 (0.991–1.033)	1.086 (1.057–1.117)	**0.974 (0.923–1.028)**	1.002 (0.987–1.017)	1.009 (0.995–1.023)
Luo et al., 2022 [105]	2022	All_ages	Guangzhou–Shenzhen–Zhuhai	1.0184 (1.0068–1.0302)	1.0154 (1.0096–1.0123)	1.0243 (1.0131–1.0356)	1.0034 (1.0010–1.0048)	**0.982 (0.52–2.14)**	1.0769 (1.0104–1.1478)
Lu et al., 2013 [87]	2013	Children	Changsha		1.021 (1.003–1.039)		1.037 (1.006–1.069)		1.026 (1.005–1.048)
Liu et al., 2020 [109]	2020	Children	NEC_7 cities	1.28 (1.09–1.51)	1.23 (1.06–1.43)	1.22 (1.05–1.42)			
Zhou et al., 2021 [110]	2021	Children	NEC_7 cities				1.13 (1.07–1.18)		
Hao et al., 2021 [53]	2021	Children	Shenyang			1.31 (1.08–1.90)	1.15 (1.02–2.23)	**0.52 (0.23–1.02)**	1.13 (0.77–2.02)
Guo et al., 2022 [104]	2022	Children	Wuhan	1.270 (1.004–1.606)	1.210 (1.042–1.405)	1.292 (1.005–1.662)		1.137 (0.973–1.329)	1.02 (0.95–1.11)

* For CO, the increase range is 1 mg/m^3. The bold values indicate the non-significant correlations between the morbidity of allergic rhinitis and air pollutants.

2.5. Definition of Potential Morbidity Risk Index

The population attributable fraction (*PAF*) is an epidemiological parameter which is used to represent the occurring proportion of morbidity/mortality that results from the specific risk factor among the whole population over the simulated domain [111]. In this study, it means the potential increased proportion of morbidity of three respiratory diseases due to exposure to outdoor pollution:

$$PAF = \frac{P_{exposure} \cdot (OR_{exposure} - 1)}{P_{exposure} \cdot (OR_{exposure} - 1) + 1} \tag{1}$$

Here, $P_{exposure}$ is the proportion of people who will be exposed to outdoor environment among the entire population, and $P_{exposure} = 0.92$ is used in this study according to questionnaire survey of Changchun.

Potential morbidity risk index of a specific respiratory disease is then calculated and its formulas are expressed as:

$$N_{i,j} = PAF \cdot N_{Specfic\_ages} \cdot \gamma_{Specfic\_ages} \tag{2}$$

$$PMRI_{Res} = N_{i,j} / \sum_{i,j=1}^{n} N_{i,j} \cdot 100 \tag{3}$$

$N_{i,j}$ is the case numbers of specific diseases for the given ages in each grid over the whole simulated domain. $OR_{exposure}$ is the scaled odds risk that corresponds the difference during exposure times between the forecasted results and the healthy values advised by the WHO, and its calculating formula is expressed as follows:

$$OR_{exposure} = exp\left(\left(\frac{lnOR}{C_{RR\_unit}}\right) \cdot C_{diff}\right) \tag{4}$$

OR is the odds risk in exposure-response function for different diseases of Chinese exposure to air pollution obtained from the local study or/and former published literatures, C_{RR_unit} is the unit concentration of exposure pollutants in exposure functions, and C_{diff} is the concentration differences between the simulated concentrations (namely, the forecasted potential exposure) and the advised healthy values by the WHO (baseline exposure).

A module written in Python was developed to conduct the time serial (hourly and daily) calculations of PMRI for each grid, pollutant and the related disease (allergic rhinitis is representatively selected in this study).

2.6. Statistical Metrics of Model Evaluation

The simulated results of WRF-VEIN-CHIMERE have been evaluated with the actual ground observations using the following statistical equations:

Correlation coefficient:

$$R = \frac{\sum_{i=1}^{n}(p_i - \bar{p})(o_i - \bar{o})}{\sqrt{\sum_{i=1}^{n}(p_i - \bar{p})^2}\sqrt{\sum_{i=1}^{n}(o_i - \bar{o})^2}} \tag{5}$$

Mean bias:

$$MB = \frac{1}{n}\sum_{i=1}^{n}(p_i - o_i) \tag{6}$$

Root mean square error:

$$RMSE = \sqrt{\frac{1}{n}\sum_{i=1}^{n}(p_i - o_i)^2} \tag{7}$$

Here, p_i and o_i are the simulated and observed values at each time and grid pair i; and $\overline{p_i}$ and $\overline{o_i}$ denote the average modeled and observed values, respectively. n is the total number of grids or timestamps. The correlation coefficient R represents the direction and strength of the linear relationship between the modeling and observation. *MB* describes the mean deviation of the simulated results from the corresponding observations. *RMSE* indicates the absolute accuracy of a model prediction and its value of 0 means a perfect model prediction.

3. Results

3.1. Accuracy Evaluation of City-Scale Simulations

3.1.1. Meteorological Variables

In order to effectively forecast the potential morbidity risk of respiratory diseases, the exposure concentrations of ambient pollutants must be accurately simulated. Serious pollution in the atmospheric environment is mainly caused by excessive anthropogenic emissions and the unfavorable diffusion conditions (i.e., regional meteorological and topographic factors). Whereas the terrain of a given area is almost impossible to change, the future variations of meteorological factors should be comprehensively evaluated.

Figure 2 illustrates the temporal (hourly) variations of major meteorological variables (temperature at 2 m, relative humidity and wind speed) among the forecasted and ground-monitored values at two local sites (Changchun Longjia International Airport and Changchun Train Station). As for the temperature, it was obvious that the daily minimum temperatures were underestimated, thus leading to the fact that the whole WRF simulations slightly underestimated the daily mean near-surface temperatures at 2 m. The WRF overestimated the relative humidity but underestimated it in July at Changchun Train Station, and overestimated the humidity at both sites in December. The WRF model shows higher correlations in high-resolution (1 km × 1 km) simulations of wind speeds in both summer and winter.

A more detailed result of the different statistical metrics was presented in Table 4 to further evaluate the model performance of WRF. The correlation coefficients between the simulated and observed hourly surface temperatures were 0.86–0.98 with negative biases ranging from −0.51−−1.39 °C. The RMSE errors showed lower values in July than December (1.97–2.38 °C to 2.16–3.05 °C). The correlation coefficients of RH in winter dropped to –0.60, and both the MB and RMSE of RH were higher in winter than summer, and the overall errors of RH was about 13.53%. The higher errors occurred in the range of higher values of humidity (RH > 80%). The averaged correlation coefficient and RMSE of wind speed were 0.72 and 1.38 m/s, respectively.

Table 4. Statistical metrics of hourly temperature (T), relative humidity (RH) and wind speed (WS) in July and December of 2021 at two sites of Changchun, northeast China.

Variables	Site	July			December		
		R	*MB*	*RMSE*	*R*	*MB*	*RMSE*
T	CLIA	0.90	0.80	1.97	0.98	−0.51	2.16
	CTS	0.86	−0.53	2.38	0.94	−1.39	3.05
RH	CLIA	0.80	2.43	10.21	0.65	10.64	14.92
	CTS	0.76	−5.91	13.23	0.56	10.22	15.75
WS	CLIA	0.72	0.10	1.20	0.79	0.31	1.22
	CTS	0.75	1.00	1.42	0.61	0.91	1.67

In this part, the model performance evaluation of WRF reveals that the optimized configuration can produce well simulated meteorological conditions for the further modeling of regional air quality at the city scale with higher resolutions (1 km × 1 km). A more

detailed exploration of model–observation mismatch will be insightful, but it is beyond the scope of this research.
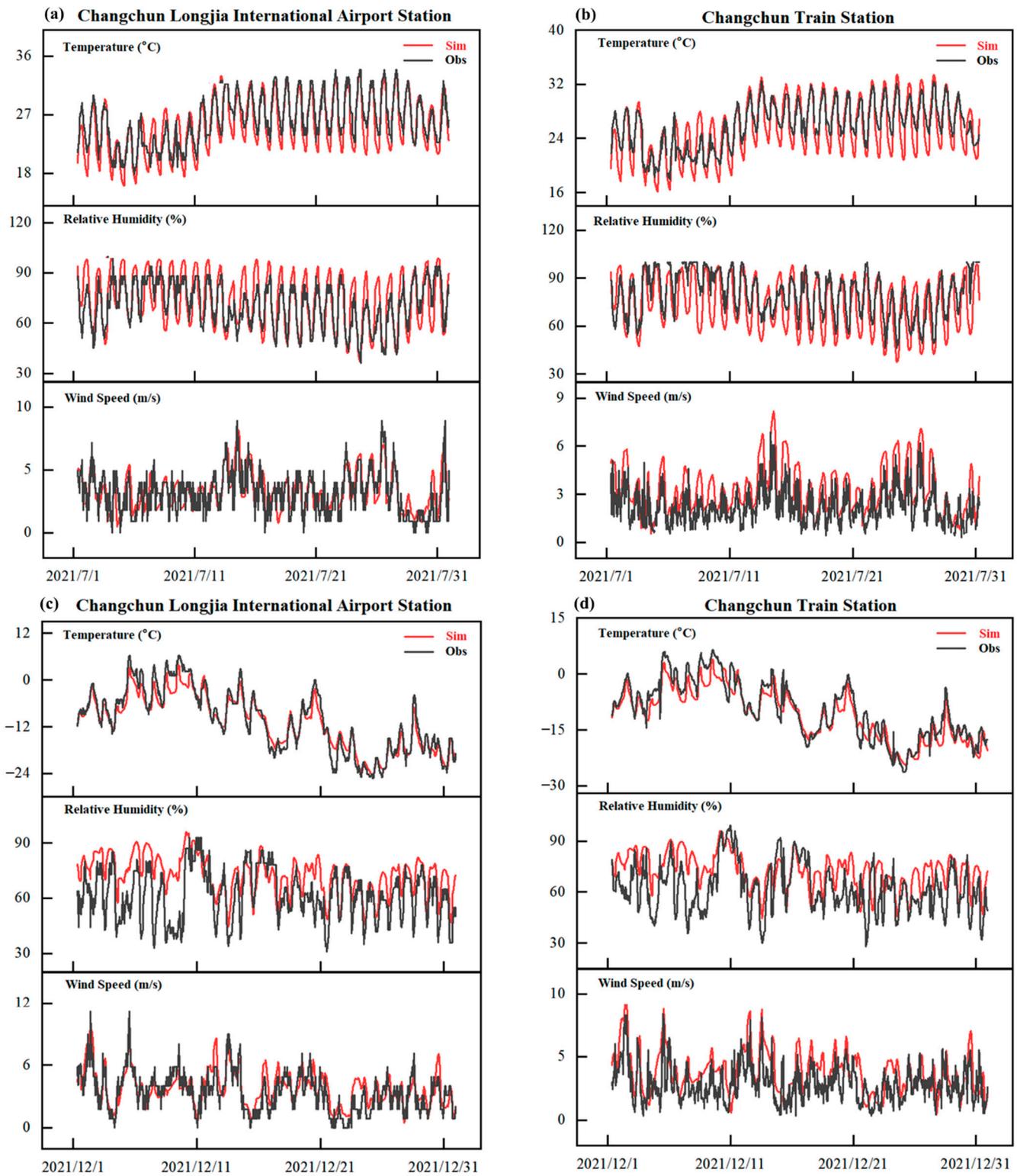

Figure 2. Time series of simulated and observed hourly air temperature at 2 m, relative humidity and wind speed at the two monitoring sites of Changchun for July and December 2021.

3.1.2. Air Quality Variables

In this study, the WRF-CHIMERE simulated the surface pollutant concentrations with enabling two different traffic emissions (default traffic emission from the MEIC inventory and the new compiled traffic emission inventory by the VEIN model), which were compared with the corresponding ground-based observations at ten sites of Changchun. As health effects of ambient pollutants on residents gradually occurred during a certain period of exposures, contrary to most previous evaluation studies models, here we compared the accumulated pollutant concentrations rather than averaged concentrations of each pollutant between the simulations and observations.

Figure 3 illustrates the spatial distribution (hindcast results) of major air quality variables with different traffic emissions in Changchun in July and December. Obviously, the overall patterns of each pollutant were not significantly changed between the scenarios of using default MEIC and updated VEIN emissions, except for PM_{10} and CO that the simulation using VEIN inventory led to higher concentrations of coarse particles and CO covering the whole southern part of Changchun (Figure 3g). Compared to the actual observation values of the site (Shuangyang) located at bottom-left corner of Figure 3b,g, the updated VEIN emissions produced better performance. Higher resolution of VEIN inventory in simulations resulted in more detailed information of spatial variations, especially for the NO_2 and O_3 (Figure 3h,j).

For the downtown areas with relatively higher pollution, the simulations with default MEIC inventory produced higher concentrations of pollutants than the simulations using updated VEIN traffic emissions. It can be explained by the fact that the VEIN model can output high resolution inventory (1 km × 1 km in this study) and produce a smaller area in each pixel to aggregate the emissions, namely, that the MEIC inventory with coarse resolution (0.25° × 0.25°) will produce higher emissions in more grids during the spatial allocation processes [78]. In the downtown area, on the other hand, the downward trend in O_3 was exactly the opposite (Figure 3e,j). A previous study based on satellite observations has demonstrated that the ozone pollution in urban areas of Changchun in summer is limited by the VOCs [112], but the nitrogen oxides dominate the depletion processes of ozone in the urban area with higher traffic emissions compared to the rural area [113].

Limited by the length of the paper, only a typical site (Site of Food Factory, SFF) was selected to conduct comprehensive statistical analysis. The time-series comparisons and scatter diagram analyses among two simulation scenarios and observation at the site of SFF with statistical metrics in July and December are presented in Figures 4 and 5, respectively.

As plotted in Figures 4 and 5, for hindcasted concentrations of $PM_{2.5}$ and PM_{10}, in both summer and winter, the correlation coefficients ranged in 0.52–0.54 at higher spatial resolution of 1 km, and the correlation coefficients showed comparative levels between simulations using the default MEIC emissions and updated VEIN emissions, but both MB and RMSE have been effectively improved. It was demonstrated that the updated high resolution traffic emissions could enhance the forecast accuracy but had no effect on the improvements of correlations. The correlation coefficients were about 0.51 and 0.57 for CO in July and December, respectively, but the scenario of using default MEIC inventory with updated traffic emissions from VEIN generated significant overestimations (underestimations) for CO compared to the observations at the site of SFF in July.
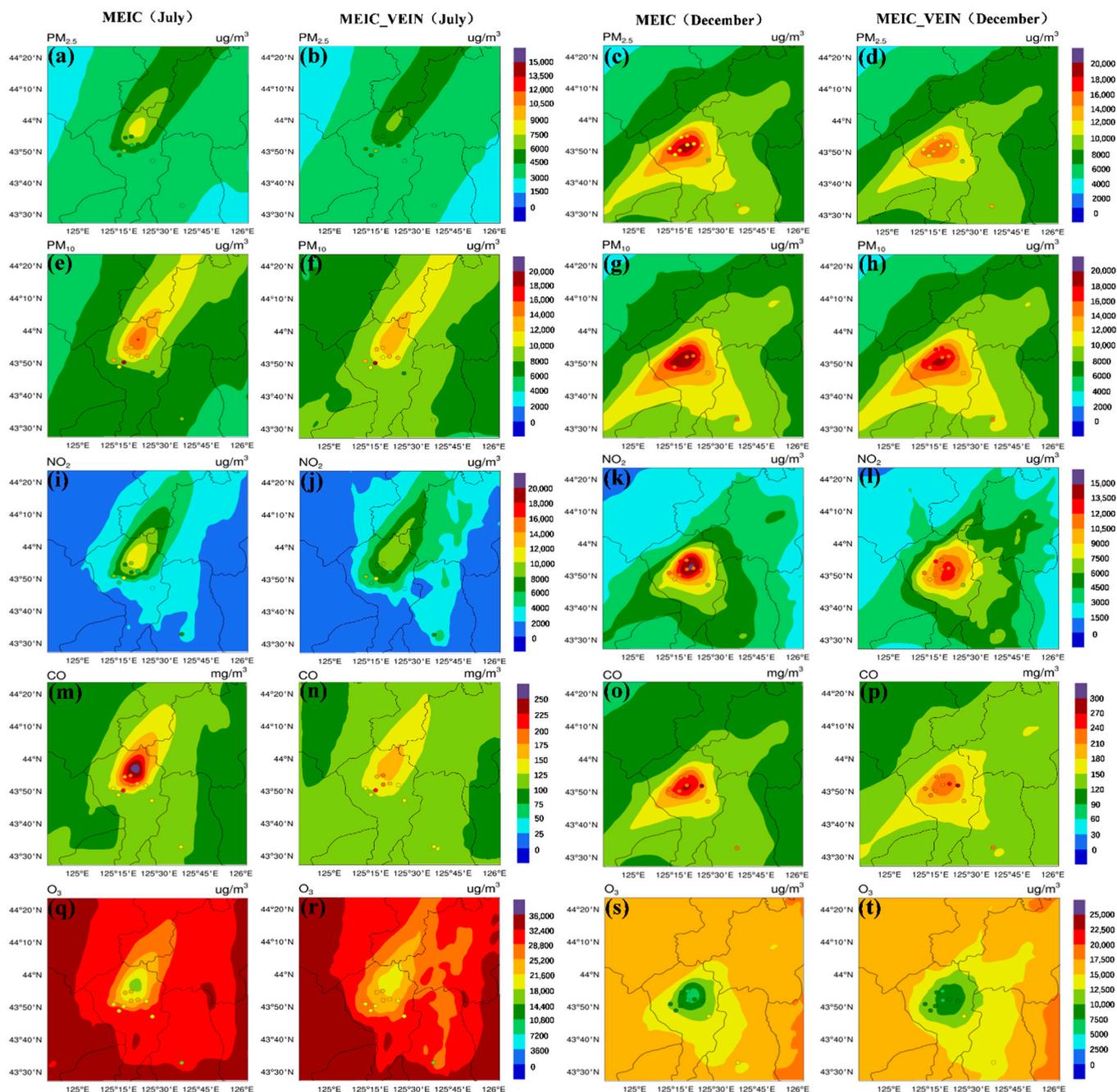
Figure 3. The accumulated pollutant concentrations of hindcast simulations with/without updated traffic emissions in July and December, ((**a**–**d**): $PM_{2.5}$; (**e**–**h**):PM_{10}; (**i**–**l**): NO_2; (**m**–**p**): CO; (**q**–**t**): O_3).

O_3 is the secondary formed pollutant and its concentration is susceptible to be influenced by the variation of precursors (NO_x and VOCs) via complicated photochemical processes [114]. Both NO_2 and O_3 can be well simulated with higher correlation coefficients (0.7–0.8) in summer and winter compared to other pollutants, and the absolute accuracy of forecast is only slightly enhanced using the updated VEIN emissions.

It was worth noting that more accurate temporal allocation profiles based on video recording and identification of vehicle types via AI algorithm were adopted in emission preprocessing steps, which resulted in the higher correlations between NO_2 and O_3 in this study. For particulates and CO, the temporal allocation profiles for different emission sectors (such as industrial and residential sources) should be further modified and checked

based on online environmental monitoring techniques in future works, and the simulation accuracy can be further theoretically improved.

Site of Food Factory

Figure 4. Comparisons between simulations with/without updated traffic emissions and observations of various pollutants with statistical metrics at the site of Food Factory from 12 July to 25 July.
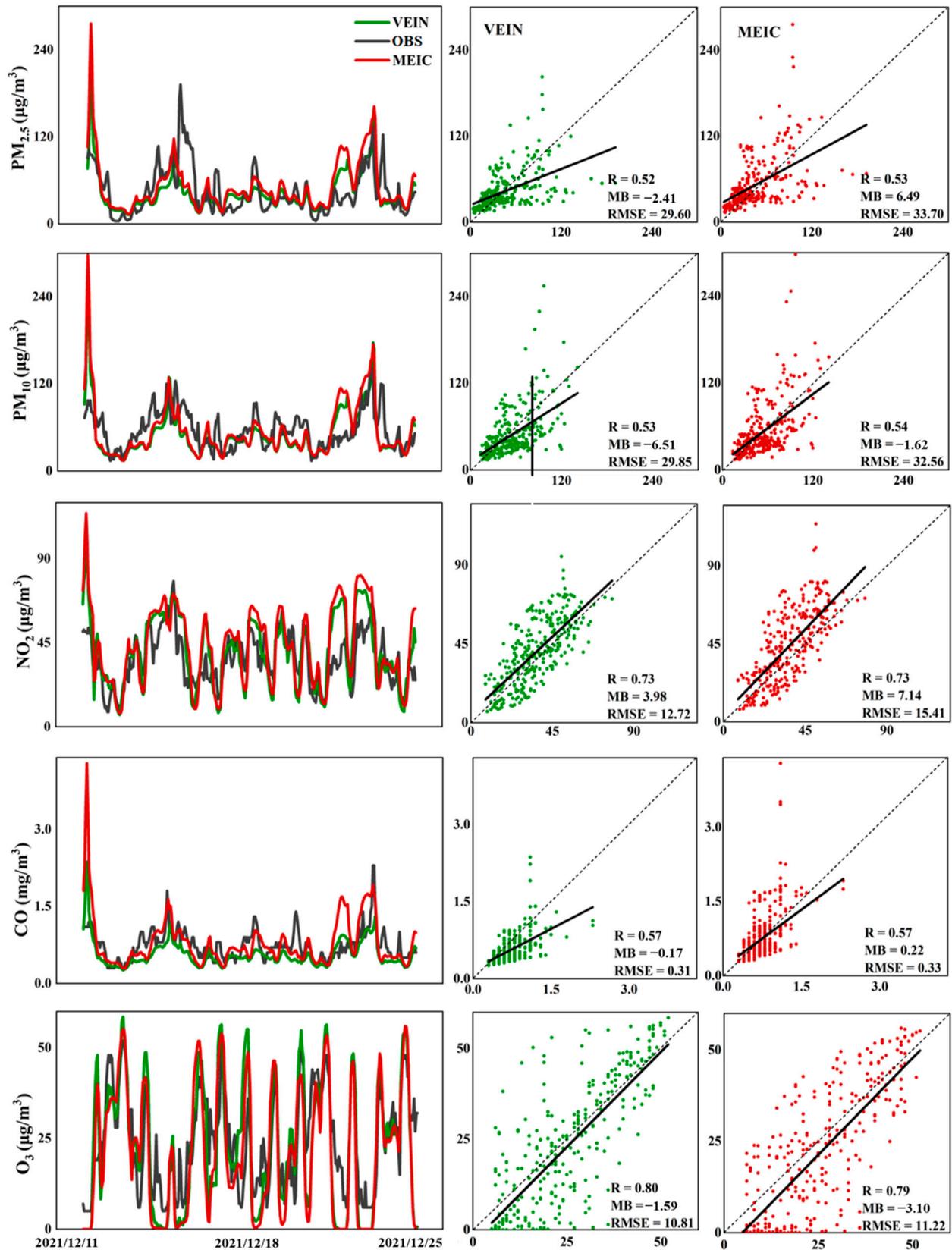
Site of Food Factory

Figure 5. Comparisons between simulations with/without updated traffic emissions and observation of various pollutants with statistical metrics at the site of Food Factory from 11 December to 24 December.

3.2. Spatiotemporal Distribution of Potential Morbidity Risk Index

It has been demonstrated in the previous evaluation sections that WRF-VEIN-CHIMERE can effectively predict future changes in outdoor pollutant concentrations. Here, we will further present the spatiotemporal distribution of calculated potential morbidity risk index at city scale with higher resolution of 1 km, which aims to further calculate the personal exposure risks combined with navigation planning data (such as Google or Baidu Maps and open-sourced OpenStreetMap) and provide corresponding health protection advice for outdoor activities of different intensities.

Figure 6 depicts the calculated spatial distributions of PMRI at specific times (namely, the typical traffic jams times in morning (8:00 a.m. LTC) and evening (17:00 p.m. LTC)) in summer and winter, respectively (More forecasted hourly PMRI results are provided in the Supplementary Materials with Graphics Interchange Format figures). In viewpoint of patients that have been diagnosed with rhinitis, the areas with higher PMRIs were mainly controlled by the leading wind directions, accumulated ambient pollution and actual dynamic traffic congestion conditions, i.e., northwestern part of Changchun on 3 July 2021 in Figure 7. In winter, the distribution pattern obviously changed and the low temperature was added as the major control factor. Therefore, the suburban and rural areas also showed certain degrees of exposure risks (PMRIs < 1.5) compared to the summer time.
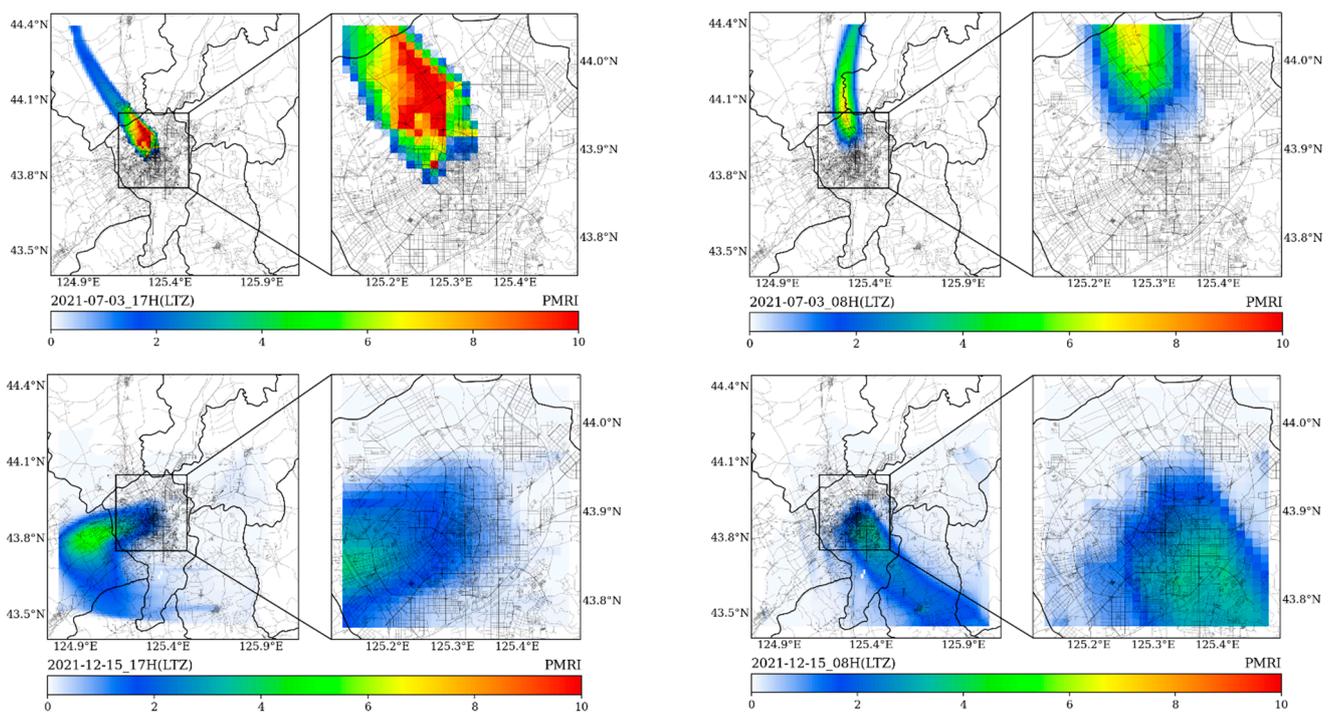

Figure 6. The spatial distributions of forecasted hourly PMRIs during typical hours (08H and 17H, LTZ) of traffic jams on 3 July and 15 December.

When comprehensively considering the spatial distribution of population, the calculated results in Figure 7 indicate the potential morbidity risks for occurrence of rhinitis in each simulated grid. The overall forecasted results can be adopted by the public health administrations and hospitals to plan and adjust the medical resources and to improve the outpatient efficiency.
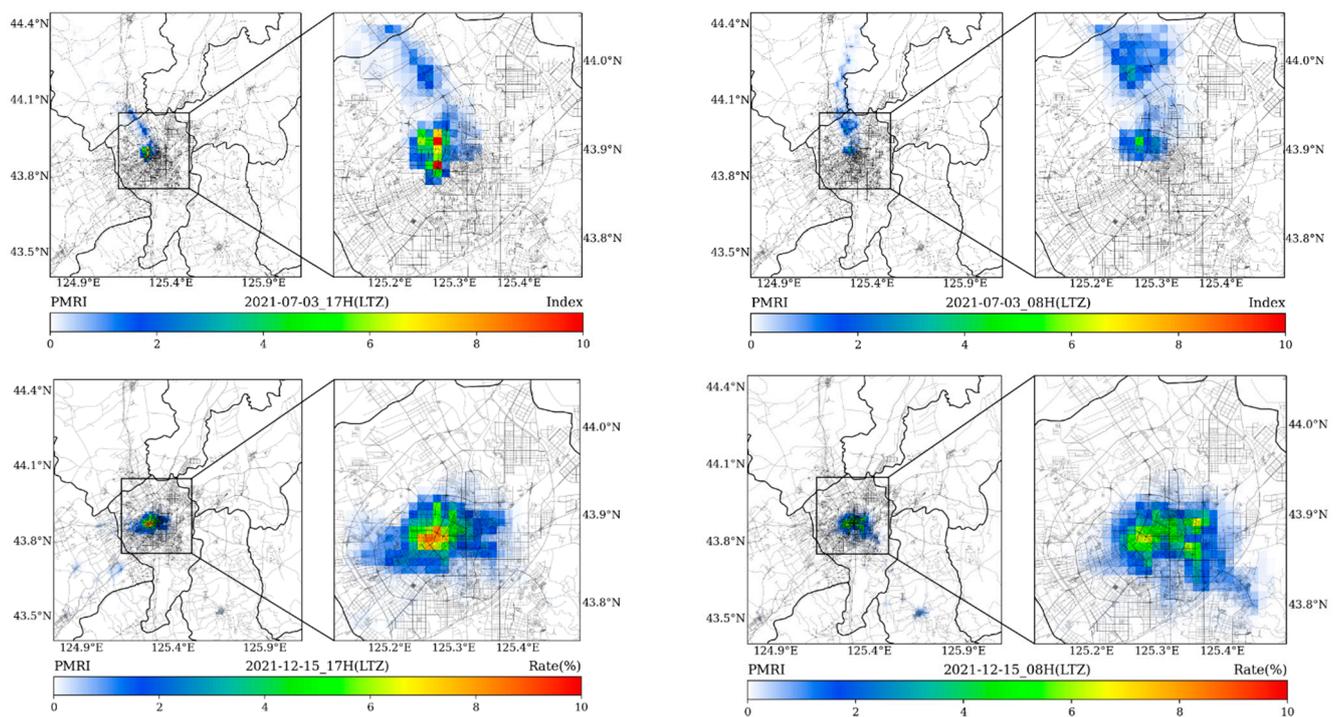
Figure 7. The spatial distributions of forecasted hourly PMRIs considering population distribution during typical hours (08H and 17H, LTZ) of traffic jams on 3 July and 15 December.

4. Discussion

Previous studies have demonstrated that the WRF model is prone to underestimating the near-surface temperature during nighttime and overestimating wind speeds in northern China [115–118]. Some studies have also indicated more complex conclusions; for example, Yan et al. [118] and Liao et al. [119] reported that underestimation or overestimation of the 2 m temperature is significantly sensitive to the selection of urban canopy schemes and data sources of green vegetation fractions in WRF in the region of Yangtze River Delta and the entire China, respectively. Schicker et al. [120] revealed that the diurnal maximum temperature is easy to be influenced by the choice of land-use datasets in WRF, but it is well simulated for both seasons with the specific configurations in Section 2.3. Similar to the study conducted by Tao et al. [121], the adoption of high-resolution grids in this study tends to reduce the uncertainties in representation of land surfaces, and this will effectively improve the model performance in simulation of meteorological fields.

Our results revealed that the adoption of high-resolution traffic emission inventory has made significant contributions to enhancing the forecast accuracy of all air quality variables in Changchun, especially for NO_2 and O_3. Previous meta-analysis based epidemiological studies have overestimated the exposure risks of allergic rhinitis due to the use of odds ratios rather than relative risks.

The first significant limitation of this study is that the local health effect estimates only considered the results from time-serious studies but lacked for the cohort studies. Until now, only limited cohort studies targeting the associations between AR and air pollution were conducted in the past; only nine papers were published in the worldwide since the year of 2013. Four out of nine cohort studies (German: Fueres et al., 2013; Netherlands: Gehring et al., 2015; Estonia: Pindus et al., 2016; Europe: Burte et al., 2020) [122–125] were conducted in Europe. Among them, Burte et al. (2018) [124] systematically investigated the association between air pollution and rhinitis incidence in two European cohorts (EGEA and ECRHS) for adults, and reported that the incident rate of allergic rhinitis is 2.34% in Europe which lower than that in China. Burte et al. (2018) [126] also reported that no clear association was found between air pollution and new incidence of allergic rhinitis both in the main analysis and the multi-pollutant model ($PM_{2.5}$, PM_{10} and NO_2). Considering

the regional differences of population and atmospheric pollution levels, the only cohort result from Europe (Burte et al., 2018) [126] for adults was also excluded from this study. In China, a total of five papers were published; three of the five papers are from Taiwan with a subtropical climate that is significantly different to that of Northeast China. In 2016, Deng et al. (2016) [49] performed the first cohort study in the mainland of China that targeted to obtain the odds ratios of allergic rhinitis when exposed to air pollutants for children aged 3–6 years in Changsha, China. Meanwhile, a study conducted in Shanghai by Liu et al. (2016) [89] also investigated the odds ratios of rhinitis and asthma for children aged 4–6. As our research target is to develop a new risk possibility index for AR patients (all ages) and health administrative sections, the results of birth cohort studies only for children from Taiwan and Changsha were excluded in our study. In short, to obtain more accurate PMRI, the corresponding effect estimates from local cohort studies should be firstly adopted rather than the time-serious or/and cross-sectional studies, and it is more reasonable using local coefficients rather than coefficients from other countries/regions.

Another major limitation of this study is that it is difficult to correlate the accumulated hourly exposures with the occurrence of rhinitis in individual patients. The personal accumulated exposure can be accomplished by trajectory tracking and mapping with recorded GPS data [127–129]. The real-time exposure dose of individual component or combines of several pollutants can be monitored via low-cost sensors/devices, such as personal exposure monitor for PM_{10}, O_3 and NO_x without GPS tracking [130], E-nose with monitoring of CO, PM_{10}, NO_2 and temperature [131], and portable personal air quality monitoring packages for $PM_{2.5}$, O_3, NO_2, NO, temperature, relative humidity and GPS recording [132,133]. The health effects and outcomes should also be made a detailed record by the participants during the 24 h personal exposure estimates [134,135]. Just for the rhinitis, the occurrence times for stuffy nose, runny nose and/or sneezing should be documented in future personal exposure estimate experiments conducted in Changchun. After the implementation of these studies, potential corresponding suggestive prevention measures (such as wearing N95 masks or/and taking antiallergic drugs) can be further taken for the forecast periods in future works.

At first, Canada proposed the Air Quality Health Index (AQHI) to communicate the health risks of multiple pollutants, but the AQHI was directly calculated by summing the excess risks from single-pollutant models, which might overestimate the effects of the pollutants. The cumulative risk index (CRI) was developed to capture the overall health risk of multiple pollutants on various cause-specific mortalities [136]. In China, the related research also demonstrated that the air pollution index (API) can be used for indicating the health risks of long-term exposure to air pollution on mortality [137]. More recently, Zhang et al. [138] emphasized the importance of temperature and considering it in building a new air health index to indicate the mortality risk.

For morbidity, various multi-pollutant AQHIs have been developed to correlate with all-cause emergence visits, hospital admissions for respiratory diseases and asthma morbidity [139–142]. In this study, we took the work one step forward and further integrated the multi-pollutants and temperature into developing a new health risk index of morbidity for allergic rhinitis based on excess risk of morbidity. Note that the excess risks were derived from time series analyses of data on hospital admissions, and the relevant cohort studies were still limited. The effects-estimates shall be updated in future works with more epidemiological studies published.

5. Conclusions

Various air quality health indices (AQHIs) have been developed and verified as a valuable health protection communication tool for the public, but the health effects mainly consider the mortality, and a possibility risk index for the morbidity of specific allergic diseases is still lacking. In this study, a city-scale health risk forecast system based on WRF-VEIN-CHIMERE for Changchun was established, and we presented the first forecasted

health-based Potential Morbidity Risk Index for allergic rhinitis patients and public health administrative sections that can be extended to other cities.

Although more and more epidemiological case- and meta-analysis studies regarding allergic rhinitis have emerged in the past decade, our analysis results revealed that the exposure risks of various air pollutants on allergic rhinitis are still under debate, especially for CO, SO_2 and O_3. Allergic rhinitis (AR) is a prevalent disease. The usage of odds ratios (ORs) may overestimate the relative risks (RRs) within the forecasted concentrations in numerical evaluations of health effects. Moreover, it is necessary to take into account the specific short-term health effects of low temperatures on the occurrence of AR at the city scale. Here, we proposed that the localized relative exposure risks should be obtained before conducting the forecast calculation of the potential morbidity risks of AR in future works.

To date, only two Europe cohort studies referring to allergic rhinitis of adults have been conducted. Burte et al. [126] reported that no clear association was found between air pollution and new occurrence of allergic rhinitis both in the main analysis and the multi-pollutant model ($PM_{2.5}$, PM_{10} and NO_2). Burte et al. [125] further demonstrated that air pollution mainly impacted on the severity of rhinitis, which is consistent with our viewpoint that air pollutants exacerbate the allergic rhinitis symptoms [43]. Thus, the forecasted hourly spatial distributions of PMRI can be used to guide the AR patients to arrange their daily activities so as to avoid acute exacerbation. It is difficult to propose corresponding preventive measures for the inevitable activity in areas with higher PMRIs, as there is a lack of quantitative relationship between personal accumulated exposures hours and the occurrence of AR, and this problem will be solved in the future. The forecasted PMRIs considering population distributions can be adopted by the public health administrations and hospitals to plan and adjust the medical resources to improve the outpatient efficiency.

Ideally, the newly developed health risk index will be further validated using local health data to confirm associations with local population-level morbidity risks.

References

1. Samet, J.; Krewski, D. Health effects associated with exposure to ambient air pollution. *J. Toxicol. Environ. Health A* **2007**, *70*, 227–242. [CrossRef]
2. Mannucci, P.M.; Franchini, M. Health Effects of Ambient Air Pollution in Developing Countries. *Int. J. Environ. Res. Public Health* **2017**, *14*, 1048. [CrossRef]
3. Curtis, L.; Rea, W.; Smith-Willis, P.; Fenyves, E.; Pan, Y. Adverse health effects of outdoor air pollutants. *Environ. Int.* **2006**, *32*, 815–830. [CrossRef]
4. Brauer, M.; Freedman, G.; Frostad, J.; van Donkelaar, A.; Martin, R.V.; Dentener, F.; van Dingenen, R.; Estep, K.; Amini, H.; Apte, J.S.; et al. Ambient Air Pollution Exposure Estimation for the Global Burden of Disease 2013. *Environ. Sci. Technol.* **2016**, *50*, 79–88. [CrossRef]
5. Querol, X.; Tobias, A.; Perez, N.; Karanasiou, A.; Amato, F.; Stafoggia, M.; Perez Garcia-Pando, C.; Ginoux, P.; Forastiere, F.; Gumy, S.; et al. Monitoring the impact of desert dust outbreaks for air quality for health studies. *Environ. Int.* **2019**, *130*, 104867. [CrossRef]
6. Jansen, K.L.; Larson, T.V.; Koenig, J.Q.; Mar, T.F.; Fields, C.; Stewart, J.; Lippmann, M. Associations between health effects and particulate matter and black carbon in subjects with respiratory disease. *Environ. Health Perspect.* **2005**, *113*, 1741–1746. [CrossRef]
7. Magalhaes, S.; Baumgartner, J.; Weichenthal, S. Impacts of exposure to black carbon, elemental carbon, and ultrafine particles from indoor and outdoor sources on blood pressure in adults: A review of epidemiological evidence. *Environ. Res.* **2018**, *161*, 345–353. [CrossRef]
8. World Health Organization. *Health Effects of Black Carbon*; WHO: Geneva, Switzerland, 2012.
9. Keuken, M.P.; Jonkers, S.; Zandveld, P.; Voogt, M.; Elshout van den, S. Elemental carbon as an indicator for evaluating the impact of traffic measures on air quality and health. *Atmos. Environ.* **2012**, *61*, 1–8. [CrossRef]
10. Han, X.; Naeher, L.P. A review of traffic-related air pollution exposure assessment studies in the developing world. *Environ. Int.* **2006**, *32*, 106–120. [CrossRef]
11. Laumbach, R.J.; Kipen, H.M. Respiratory health effects of air pollution: Update on biomass smoke and traffic pollution. *J. Allergy Clin. Immunol.* **2012**, *129*, 3–11. [CrossRef]
12. Stenson, C.; Wheeler, A.J.; Carver, A.; Donaire-Gonzalez, D.; Alvarado-Molina, M.; Nieuwenhuijsen, M.; Tham, R. The impact of Traffic-Related air pollution on child and adolescent academic Performance: A systematic review. *Environ. Int.* **2021**, *155*, 106696. [CrossRef] [PubMed]
13. Wong, Y.J.; Shiu, H.Y.; Chang, J.H.H.; Ooi, M.C.G.; Li, H.H.; Homma, R.; Shimizu, Y.; Pei-Te, C.; Maneechot, L.; Sulaiman, N.M.N. Spatiotemporal impact of COVID-19 on Taiwan air quality in the absence of a lockdown: Influence of urban public transportation use and meteorological conditions. *J. Clean. Prod.* **2022**, *365*, 132893. [CrossRef] [PubMed]
14. Zhang, Q.; Jiang, X.J.; Tong, D.; Davis, S.J.; Zhao, H.Y.; Geng, G.N.; Feng, T.; Zheng, B.; Lu, Z.F.; Streets, D.G.; et al. Transboundary health impacts of transported global air pollution and international trade. *Nature* **2017**, *543*, 705–709. [CrossRef]
15. Vohra, K.; Vodonos, A.; Schwartz, J.; Marais, E.A.; Sulprizio, M.P.; Mickley, L.J. Global mortality from outdoor fine particle pollution generated by fossil fuel combustion: Results from GEOS-Chem. *Environ. Res.* **2021**, *195*, 110754. [CrossRef]
16. Selin, N.E.; Wu, S.; Nam, K.M.; Reilly, J.M.; Paltsev, S.; Prinn, R.G.; Webster, M.D. Global health and economic impacts of future ozone pollution. *Environ. Res. Lett.* **2009**, *4*, 044014. [CrossRef]
17. Likhvar, V.N.; Pascal, M.; Markakis, K.; Colette, A.; Hauglustaine, D.; Valari, M.; Klimont, Z.; Medina, S.; Kinney, P. A multi-scale health impact assessment of air pollution over the 21st century. *Sci. Total Environ.* **2015**, *514*, 439–449. [CrossRef] [PubMed]
18. Fann, N.; Fulcher, C.M.; Hubbell, B.J. The influence of location, source, and emission type in estimates of the human health benefits of reducing a ton of air pollution. *Air Qual. Atmos. Health* **2009**, *2*, 169–176. [CrossRef]
19. Hu, J.; Li, X.; Huang, L.; Ying, Q.; Zhang, Q.; Zhao, B.; Wang, S.; Zhang, H. Ensemble prediction of air quality using the WRF/CMAQ model system for health effect studies in China. *Atmos. Chem. Phys.* **2017**, *17*, 13103–13118. [CrossRef]
20. Wang, Z.; Li, J.; Mu, X.; Zhao, L.; Gu, C.; Gao, H.; Ma, J.; Mao, X.; Huang, T. A WRF-CMAQ modeling of atmospheric PAH cycling and health risks in the heavy petrochemical industrialized Lanzhou valley, Northwest China. *J. Clean. Prod.* **2021**, *291*, 125989. [CrossRef]
21. Hao, H.; Chang, H.H.; Holmes, H.A.; Mulholland, J.A.; Klein, M.; Darrow, L.A.; Strickland, M.J. Air Pollution and Preterm Birth in the U.S. State of Georgia (2002–2006): Associations with Concentrations of 11 Ambient Air Pollutants Estimated by Combining Community Multiscale Air Quality Model (CMAQ) Simulations with Stationary Monitor Measurements. *Environ. Health Perspect.* **2016**, *124*, 875–880. [CrossRef]
22. Gao, M.; Guttikunda, S.K.; Carmichael, G.R.; Wang, Y.; Liu, Z.; Stanier, C.O.; Saide, P.E.; Yu, M. Health impacts and economic losses assessment of the 2013 severe haze event in Beijing area. *Sci. Total Environ.* **2015**, *511*, 553–561. [CrossRef] [PubMed]
23. Ballesteros-Gonzalez, K.; Sullivan, A.P.; Morales-Betancourt, R. Estimating the air quality and health impacts of biomass burning in northern South America using a chemical transport model. *Sci. Total Environ.* **2020**, *739*, 139755. [CrossRef] [PubMed]
24. Kryza, M.; Werner, M.; Dudek, J.; Dore, A.J. The Effect of Emission Inventory on Modelling of Seasonal Exposure Metrics of Particulate Matter and Ozone with the WRF-Chem Model for Poland. *Sustainability* **2020**, *12*, 5414. [CrossRef]
25. Thompson, T.M.; Saari, R.K.; Selin, N.E. Air quality resolution for health impact assessment: Influence of regional characteristics. *Atmos. Chem. Phys.* **2014**, *14*, 969–978. [CrossRef]

26. Parvez, F.; Wagstrom, K. Impact of regional versus local resolution air quality modeling on particulate matter exposure health impact assessment. *Air Qual. Atmos. Health* **2020**, *13*, 271–279. [CrossRef]

27. Mauzerall, D.L.; Sultan, B.; Kim, N.; Bradford, D.F. Nox emissions from large point sources: Variability in ozone production, resulting health damages and economic costs. *Atmos. Environ.* **2005**, *39*, 2851–2866. [CrossRef]

28. Fann, N.; Baker, K.R.; Fulcher, C.M. Characterizing the PM2.5-related health benefits of emission reductions for 17 industrial, area and mobile emission sectors across the U.S. *Environ. Int.* **2012**, *49*, 141–151. [CrossRef]

29. Guttikunda, S.K.; Jawahar, P. Evaluation of Particulate Pollution and Health Impacts from Planned Expansion of Coal-Fired Thermal Power Plants in India Using WRF-CAMx Modeling System. *Aerosol Air Qual. Res.* **2018**, *18*, 3187–3201. [CrossRef]

30. Bouscasse, H.; Gabet, S.; Kerneis, G.; Provent, A.; Rieux, C.; Ben Salem, N.; Dupont, H.; Troude, F.; Mathy, S.; Slama, R. Designing local air pollution policies focusing on mobility and heating to avoid a targeted number of pollution-related deaths: Forward and backward approaches combining air pollution modeling, health impact assessment and cost-benefit analysis. *Environ. Int.* **2022**, *159*, 107030. [CrossRef]

31. Valari, M.; Menut, L.; Chatignoux, E. Using a chemistry transport model to account for the spatial variability of exposure concentrations in epidemiologic air pollution studies. *J. Air Waste Manag. Assoc.* **2011**, *61*, 164–179. [CrossRef] [PubMed]

32. Kiesewetter, G.; Schoepp, W.; Heyes, C.; Amann, M. Modelling PM2.5 impact indicators in Europe: Health effects and legal compliance. *Environ. Model. Softw.* **2015**, *74*, 201–211. [CrossRef]

33. Sanyal, S.; Rochereau, T.; Maesano, C.N.; Com-Ruelle, L.; Annesi-Maesano, I. Long-Term Effect of Outdoor Air Pollution on Mortality and Morbidity: A 12-Year Follow-Up Study for Metropolitan France. *Int. J. Environ. Res. Public Health* **2018**, *15*, 2487. [CrossRef] [PubMed]

34. Rivas, E.; Santiago, J.L.; Lechon, Y.; Martin, F.; Arino, A.; Pons, J.J.; Santamaria, J.M. CFD modelling of air quality in Pamplona City (Spain): Assessment, stations spatial representativeness and health impacts valuation. *Sci. Total Environ.* **2019**, *649*, 1362–1380. [CrossRef]

35. Buonocore, J.J.; Dong, X.; Spengler, J.D.; Fu, J.S.; Levy, J.I. Using the Community Multiscale Air Quality (CMAQ) model to estimate public health impacts of $PM_{2.5}$ from individual power plants. *Environ. Int.* **2014**, *68*, 200–208. [CrossRef]

36. Guttikunda, S.K.; Jawahar, P. Atmospheric emissions and pollution from the coal-fired thermal power plants in India. *Atmos. Environ.* **2014**, *92*, 449–460. [CrossRef]

37. Strasert, B.; Teh, S.C.; Cohan, D.S. Air quality and health benefits from potential coal power plant closures in Texas. *J. Air Waste Manag. Assoc.* **2019**, *69*, 333–350. [CrossRef]

38. Fann, N.; Baker, K.R.; Chan, E.A.W.; Eyth, A.; Macpherson, A.; Miller, E.; Snyder, J. Assessing Human Health $PM_{2.5}$ and Ozone Impacts from U.S. Oil and Natural Gas Sector Emissions in 2025. *Environ. Sci. Technol.* **2018**, *52*, 8095–8103. [CrossRef]

39. Arunachalam, S.; Wang, B.; Davis, N.; Baek, B.H.; Levy, J.I. Effect of chemistry-transport model scale and resolution on population exposure to $PM_{2.5}$ from aircraft emissions during landing and takeoff. *Atmos. Environ.* **2011**, *45*, 3294–3300. [CrossRef]

40. Li, Y.; Henze, D.K.; Jack, D.; Kinney, P.L. The influence of air quality model resolution on health impact assessment for fine particulate matter and its components. *Air Qual. Atmos. Health* **2016**, *9*, 51–68. [CrossRef]

41. Jiang, X.; Yoo, E.H. The importance of spatial resolutions of Community Multiscale Air Quality (CMAQ) models on health impact assessment. *Sci. Total Environ.* **2018**, *627*, 1528–1543. [CrossRef] [PubMed]

42. Kirwa, K.; Szpiro, A.A.; Sheppard, L.; Sampson, P.D.; Wang, M.; Keller, J.P.; Young, M.T.; Kim, S.Y.; Larson, T.V.; Kaufman, J.D. Fine-Scale Air Pollution Models for Epidemiologic Research: Insights from Approaches Developed in the Multi-ethnic Study of Atherosclerosis and Air Pollution (MESA Air). *Curr. Environ. Health Rep.* **2021**, *8*, 113–126. [CrossRef] [PubMed]

43. Teng, B.; Zhang, X.; Yi, C.; Zhang, Y.; Ye, S.; Wang, Y.; Tong, D.Q.; Lu, B. The Association between Ambient Air Pollution and Allergic Rhinitis: Further Epidemiological Evidence from Changchun, Northeastern China. *Int. J. Environ. Res. Public Health* **2017**, *14*, 226. [CrossRef]

44. Eguiluz-Gracia, I.; Mathioudakis, A.G.; Bartel, S.; Vijverberg, S.J.H.; Fuertes, E.; Comberiati, P.; Cai, Y.S.; Tomazic, P.V.; Diamant, Z.; Vestbo, J.; et al. The need for clean air: The way air pollution and climate change affect allergic rhinitis and asthma. *Allergy* **2020**, *75*, 2170–2184. [CrossRef] [PubMed]

45. Li, S.; Wu, W.; Wang, G.; Zhang, X.; Guo, Q.; Wang, B.; Cao, S.; Yan, M.; Pan, X.; Xue, T.; et al. Association between exposure to air pollution and risk of allergic rhinitis: A systematic review and meta-analysis. *Environ. Res.* **2022**, *205*, 112472. [CrossRef]

46. Anenberg, S.C.; Mohegh, A.; Goldberg, D.L.; Kerr, G.H.; Brauer, M.; Burkart, K.; Hystad, P.; Larkin, A.; Wozniak, S.; Lamsal, L. Long-term trends in urban NO_2 concentrations and associated paediatric asthma incidence: Estimates from global datasets. *Lancet Planet. Health* **2022**, *6*, e49–e58. [CrossRef]

47. Pekkanen, J.; Pearce, N. Defining asthma in epidemiological studies. *Eur. Respir. J.* **1999**, *14*, 951–957. [CrossRef]

48. Jung, D.Y.; Leem, J.H.; Kim, H.C.; Kim, J.H.; Hwang, S.S.; Lee, J.Y.; Kim, B.J.; Hong, Y.C.; Hong, S.J.; Kwon, H.J. Effect of Traffic-Related Air Pollution on Allergic Disease: Results of the Children's Health and Environmental Research. *Allergy Asthma Immunol. Res.* **2015**, *7*, 359–366. [CrossRef]

49. Deng, Q.; Lu, C.; Yu, Y.; Li, Y.; Sundell, J.; Norback, D. Early life exposure to traffic-related air pollution and allergic rhinitis in preschool children. *Respir. Med.* **2016**, *121*, 67–73. [CrossRef] [PubMed]

50. Khreis, H.; Kelly, C.; Tate, J.; Parslow, R.; Lucas, K.; Nieuwenhuijsen, M. Exposure to traffic-related air pollution and risk of development of childhood asthma: A systematic review and meta-analysis. *Environ. Int.* **2017**, *100*, 1–31. [CrossRef]

51. Heinrich, J.; Wichmann, H.E. Traffic related pollutants in Europe and their effect on allergic disease. *Curr. Opin. Allergy Clin. Immunol.* **2004**, *4*, 341–348. [CrossRef]

52. Bowatte, G.; Lodge, C.; Lowe, A.J.; Erbas, B.; Perret, J.; Abramson, M.J.; Matheson, M.; Dharmage, S.C. The influence of childhood traffic-related air pollution exposure on asthma, allergy and sensitization: A systematic review and a meta-analysis of birth cohort studies. *Allergy* **2015**, *70*, 245–256. [PubMed]

53. Hao, S.; Yuan, F.; Pang, P.; Yang, B.; Jiang, X.; Yan, A.J.E.H.; Medicine, P. Early childhood traffic-related air pollution and risk of allergic rhinitis at 2–4 years of age modification by family stress and male gender: A case-control study in Shenyang, China. *Environ. Health Prev. Med.* **2021**, *26*, 1–11. [CrossRef] [PubMed]

54. Zou, Q.Y.; Shen, Y.; Ke, X.; Hong, S.L.; Kang, H.Y. Exposure to air pollution and risk of prevalence of childhood allergic rhinitis: A meta-analysis. *Int. J. Pediatr. Otorhinolaryngol.* **2018**, *112*, 82–90. [CrossRef] [PubMed]

55. Hu, Y.; Xu, Z.; Jiang, F.; Li, S.; Liu, S.; Wu, M.; Yan, C.; Tan, J.; Yu, G.; Hu, Y.; et al. Relative impact of meteorological factors and air pollutants on childhood allergic diseases in Shanghai, China. *Sci. Total Environ.* **2020**, *706*, 135975. [CrossRef]

56. Jia, X.; Shen, Z.; Liu, R.; Han, Y.; Yang, Y.; Chen, Q.; Duan, N. Association of fine particulate matter to allergic rhinitis: A systematic review and meta-analysis. *Eur. J. Inflamm.* **2022**, *20*, 1721727X221089839. [CrossRef]

57. Gasana, J.; Dillikar, D.; Mendy, A.; Forno, E.; Ramos Vieira, E. Motor vehicle air pollution and asthma in children: A meta-analysis. *Environ. Res.* **2012**, *117*, 36–45. [CrossRef]

58. Anderson, H.R.; Favarato, G.; Atkinson, R.W. Long-term exposure to air pollution and the incidence of asthma: Meta-analysis of cohort studies. *Air Qual. Atmos. Health* **2011**, *6*, 47–56. [CrossRef]

59. Zheng, X.Y.; Ding, H.; Jiang, L.N.; Chen, S.W.; Zheng, J.P.; Qiu, M.; Zhou, Y.X.; Chen, Q.; Guan, W.J. Association between Air Pollutants and Asthma Emergency Room Visits and Hospital Admissions in Time Series Studies: A Systematic Review and Meta-Analysis. *PLoS ONE* **2015**, *10*, e0138146. [CrossRef]

60. Zhang, S.; Li, G.; Tian, L.; Guo, Q.; Pan, X. Short-term exposure to air pollution and morbidity of COPD and asthma in East Asian area: A systematic review and meta-analysis. *Environ. Res.* **2016**, *148*, 15–23.

61. Han, K.; Ran, Z.; Wang, X.; Wu, Q.; Zhan, N.; Yi, Z.; Jin, T. Traffic-related organic and inorganic air pollution and risk of development of childhood asthma: A meta-analysis. *Environ. Res.* **2021**, *194*, 110493. [CrossRef]

62. Orellano, P.; Quaranta, N.; Reynoso, J.; Balbi, B.; Vasquez, J. Effect of outdoor air pollution on asthma exacerbations in children and adults: Systematic review and multilevel meta-analysis. *PLoS ONE* **2017**, *12*, e0174050. [CrossRef]

63. Lai, H.K.; Tsang, H.; Wong, C.M. Meta-analysis of adverse health effects due to air pollution in Chinese populations. *BMC Public Health* **2013**, *13*, 360. [CrossRef]

64. Kindzierski, W.; Young, S.; Meyer, T.; Dunn, J. Evaluation of a meta-analysis of ambient air quality as a risk factor for asthma exacerbation. *J. Respir.* **2021**, *1*, 173–196. [CrossRef]

65. Graudenz, G.S.; Landgraf, R.G.; Jancar, S.; Tribess, A.; Fonseca, S.G.; Fae, K.C.; Kalil, J. The role of allergic rhinitis in nasal responses to sudden temperature changes. *J. Allergy Clin. Immunol.* **2006**, *118*, 1126–1132. [CrossRef]

66. Xu, M.; Ke, P.; Chen, R.; Hu, P.; Liu, B.; Hou, J.; Ke, L. Association of temperature variability with the risk of initial outpatient visits for allergic rhinitis: A time-series study in Changchun. *Environ. Sci. Pollut. Res. Int.* **2022**, *29*, 27222–27231. [CrossRef]

67. Jo, E.J.; Lee, W.S.; Jo, H.Y.; Kim, C.H.; Eom, J.S.; Mok, J.H.; Kim, M.H.; Lee, K.; Kim, K.U.; Lee, M. Effects of particulate matter on respiratory disease and the impact of meteorological factors in Busan, Korea. *Respir. Med.* **2017**, *124*, 79–87. [CrossRef]

68. Duan, J.; Wang, X.; Zhao, D.; Wang, S.; Bai, L.; Cheng, Q.; Gao, J.; Xu, Z.; Zhang, Y.; Zhang, H.; et al. Risk effects of high and low relative humidity on allergic rhinitis: Time series study. *Environ. Res.* **2019**, *173*, 373–378. [CrossRef]

69. Lin, G.C.; Zacharek, M.A. Climate change and its impact on allergic rhinitis and other allergic respiratory diseases. *Curr. Opin. Otolaryngol. Head Neck Surg.* **2012**, *20*, 188–193. [CrossRef]

70. Wang, X.; Cheng, J.; Ling, L.; Su, H.; Zhao, D.; Ni, H. Impact of temperature variability on childhood allergic rhinitis in a subtropical city of China. *BMC Public Health* **2020**, *20*, 1418. [CrossRef]

71. Wang, J.; Lu, M.; An, Z.; Jiang, J.; Li, J.; Wang, Y.; Du, S.; Zhang, X.; Zhou, H.; Cui, J.; et al. Associations between air pollution and outpatient visits for allergic rhinitis in Xinxiang, China. *Environ. Sci. Pollut. Res. Int.* **2020**, *27*, 23565–23574. [CrossRef]

72. Wu, R.; Guo, Q.; Fan, J.; Guo, C.; Wang, G.; Wu, W.; Xu, J. Association between air pollution and outpatient visits for allergic rhinitis: Effect modification by ambient temperature and relative humidity. *Sci. Total Environ.* **2022**, *821*, 152960. [CrossRef]

73. Gao, J.; Lu, M.; Sun, Y.; Wang, J.; An, Z.; Liu, Y.; Li, J.; Jia, Z.; Wu, W.; Song, J. Changes in ambient temperature increase hospital outpatient visits for allergic rhinitis in Xinxiang, China. *BMC Public Health* **2021**, *21*, 600. [CrossRef] [PubMed]

74. Hsieh, S.P.; Hsieh, C.J.; Tseng, C.C.; Yiin, L.M. Allergic Rhinitis: Association with Air Pollution and Weather Changes, and Comparison with That of Allergic Conjunctivitis in Taiwan. *Atmosphere* **2020**, *11*, 1152. [CrossRef]

75. Kim, H.; Kim, H.; Lee, J.T. Assessing the cold temperature effect on hospital visit by allergic rhinitis in Seoul, Korea. *Sci. Total Environ.* **2018**, *633*, 938–945. [CrossRef] [PubMed]

76. Mailler, S.; Menut, L.; Khvorostyanov, D.; Valari, M.; Couvidat, F.; Siour, G.; Turquety, S.; Briant, R.; Tuccella, P.; Bessagnet, B. CHIMERE-2017: From urban to hemispheric chemistry-transport modeling. *Geosci. Model Dev.* **2017**, *10*, 2397–2423. [CrossRef]

77. Ibarra-Espinosa, S.; Ynoue, R.; O'Sullivan, S.; Pebesma, E.; Andrade, M.d.f.; Osses, M. VEIN v0. 2.2: An R package for bottom-up vehicular emissions inventories. *Geosci. Model Dev.* **2018**, *11*, 2209–2229. [CrossRef]

78. Ibarra-Espinosa, S.; Zhang, X.; Xiu, A.; Gao, C.; Wang, S.; Ba, Q.; Gao, C.; Chen, W. A comprehensive spatial and temporal vehicular emissions for northeast China. *Atmos. Environ.* **2021**, *244*, 117952. [CrossRef]

79. Lipfert, F. An Assessment of air pollution exposure information for health studies. *Atmosphere* **2015**, *6*, 1736–1752. [CrossRef]

80. George, A.; Stead, T.S.; Ganti, L. What's the risk: Differentiating risk ratios, odds ratios, and hazard ratios? *Cureus* **2020**, *12*, e10047. [CrossRef]

81. Brook, R.D.; Jerreft, M.; Brook, J.R.; Bard, R.L.; Finkelstein, M.M. The relationship between diabetes mellitus and traffic-related air pollution. *J. Occup. Environ. Med.* **2008**, *50*, 32–38. [CrossRef]

82. Lee, J. Odds ratio or relative risk for cross-sectional data? *Int. J. Epidemiol.* **1994**, *23*, 201–203. [CrossRef] [PubMed]

83. Lin, L.; Li, T.; Sun, M.; Liang, Q.; Ma, Y.; Wang, F.; Duan, J.; Sun, Z. Effect of particulate matter exposure on the prevalence of allergic rhinitis in children: A systematic review and meta-analysis. *Chemosphere* **2021**, *268*, 128841. [CrossRef] [PubMed]

84. Zhang, S.; Fu, Q.; Wang, S.; Jin, X.; Tan, J.; Ding, K.; Zhang, Q.; Li, X. Association between air pollution and the prevalence of allergic rhinitis in Chinese children: A systematic review and meta-analysis. *Allergy Asthma Proc.* **2022**, *43*, e47–e57. [CrossRef] [PubMed]

85. Hwang, B.F.; Jaakkola, J.J.; Lee, Y.L.; Lin, Y.C.; Leon Guo, Y.L. Relation between air pollution and allergic rhinitis in Taiwanese schoolchildren. *Respir. Res.* **2006**, *7*, 1–7. [CrossRef] [PubMed]

86. Dong, G.H.; Chen, T.; Liu, M.M.; Wang, D.; Ma, Y.N.; Ren, W.H.; Lee, Y.L.; Zhao, Y.D.; He, Q.C. Gender differences and effect of air pollution on asthma in children with and without allergic predisposition: Northeast Chinese children health study. *PLoS ONE* **2011**, *6*, e22470. [CrossRef] [PubMed]

87. Lu, C.; Deng, Q.; Ou, C.; Liu, W.; Sundell, J. Effects of ambient air pollution on allergic rhinitis among preschool children in Changsha, China. *Chin. Sci. Bull.* **2013**, *58*, 4252–4258. [CrossRef]

88. Liu, M.M.; Wang, D.; Zhao, Y.; Liu, Y.Q.; Huang, M.M.; Liu, Y.; Sun, J.; Ren, W.H.; Zhao, Y.D.; He, Q.C. Effects of outdoor and indoor air pollution on respiratory health of Chinese children from 50 kindergartens. *J. Epidemiol.* **2013**, *23*, 280–287. [CrossRef]

89. Liu, W.; Huang, C.; Hu, Y.; Fu, Q.Y.; Zou, Z.J.; Sun, C.J.; Shen, L.; Wang, X.Y.; Cai, J.; Pan, J. Associations of gestational and early life exposures to ambient air pollution with childhood respiratory diseases in Shanghai, China: A retrospective cohort study. *Environ. Int.* **2016**, *92–93*, 284–293. [CrossRef]

90. Wang, I.J.; Tung, T.H.; Tang, C.S.; Zhao, Z.H. Allergens, air pollutants, and childhood allergic diseases. *Int. J. Hyg. Environ. Health* **2016**, *219*, 66–71. [CrossRef]

91. Chung, H.Y.; Hsieh, C.J.; Tseng, C.C.; Yiin, L.M. Association between the first occurrence of allergic rhinitis in preschool children and air pollution in Taiwan. *Int. J. Environ. Res. Public Health* **2016**, *13*, 268. [CrossRef]

92. Li, R.L.; Ho, Y.C.; Luo, C.W.; Lee, S.S.; Kuan, Y.H. Influence of PM$_{2.5}$ exposure level on the association between Alzheimer's Disease and allergic rhinitis: A National Population-Based Cohort Study. *Int. J. Environ. Res. Public Health* **2019**, *16*, 3357. [CrossRef] [PubMed]

93. Chen, C.C.; Chiu, H.F.; Yang, C.Y. Air pollution exposure and daily clinical visits for allergic rhinitis in a subtropical city: Taipei, Taiwan. *J. Toxicol. Environ. Health Part A* **2016**, *79*, 494–501. [CrossRef] [PubMed]

94. Lin, Z.; Chen, R.; Norback, D.; Liu, C.; Kan, H.; Deng, Q.; Huang, C.; Hu, Y.; Zou, Z.; Liu, W. The effects of PM$_{2.5}$ on asthmatic and allergic diseases or symptoms in preschool children of six Chinese cities, based on China, Children, Homes and Health (CCHH) project. *Environ. Pollut.* **2018**, *232*, 329–337.

95. Norbäck, D.; Lu, C.; Wang, J.; Zhang, Y.; Li, B.; Zhao, Z.; Huang, C.; Zhang, X.; Qian, H.; Sun, Y. Asthma and rhinitis among Chinese children–indoor and outdoor air pollution and indicators of socioeconomic status (SES). *Environ. Int.* **2018**, *115*, 1–8. [CrossRef]

96. Huang, Q.; Ren, Y.; Liu, Y.; Liu, S.; Liu, F.; Li, X.; Li, B.; Hou, Y.; Lu, Y.; Li, S. Associations of gestational and early life exposure to air pollution with childhood allergic rhinitis. *Atmos. Environ.* **2019**, *200*, 190–196. [CrossRef]

97. Liu, W.; Cai, J.; Fu, Q.; Zou, Z.; Sun, C.; Zhang, J.; Huang, C. Associations of ambient air pollutants with airway and allergic symptoms in 13,335 preschoolers in Shanghai, China. *Chemosphere* **2020**, *252*, 126600. [CrossRef]

98. Wang, J.; Zhang, Y.; Li, B.; Zhao, Z.; Huang, C.; Zhang, X.; Deng, Q.; Lu, C.; Qian, H.; Yang, X. Asthma and allergic rhinitis among young parents in China in relation to outdoor air pollution, climate and home environment. *Sci. Total Environ.* **2021**, *751*, 141734. [CrossRef]

99. Chen, Z.; Cui, L.; Cui, X.; Li, X.; Yu, K.; Yue, K.; Dai, Z.; Zhou, J.; Jia, G.; Zhang, J. The association between high ambient air pollution exposure and respiratory health of young children: A cross sectional study in Jinan, China. *Sci. Total Environ.* **2019**, *656*, 740–749. [CrossRef]

100. Zhang, F.; Wang, W.; Lv, J.; Krafft, T.; Xu, J. Time-series studies on air pollution and daily outpatient visits for allergic rhinitis in Beijing, China. *Sci. Total Environ.* **2011**, *409*, 2486–2492. [CrossRef]

101. Zhang, F.; Xu, J.; Wang, L.; Lu, J.; Li, Y.; Ni, Y.; Wang, W.; Krafft, T. Air quality, patterns and otolaryngology health effects of air pollutants in Beijing in 2013. *Aerosol Air Qual. Res.* **2016**, *16*, 1464–1472. [CrossRef]

102. Chu, H.; Xin, J.; Yuan, Q.; Wang, M.; Cheng, L.; Zhang, Z.; Lu, M. The effects of particulate matters on allergic rhinitis in Nanjing, China. *Environ. Sci. Pollut. Res.* **2019**, *26*, 11452–11457. [CrossRef] [PubMed]

103. Wang, M.; Wang, S.; Wang, X.; Tian, Y.; Wu, Y.; Cao, Y.; Song, J.; Wu, T.; Hu, Y. The association between PM$_{2.5}$ exposure and daily outpatient visits for allergic rhinitis: Evidence from a seriously air-polluted environment. *Int. J. Biometeorol.* **2020**, *64*, 139–144. [CrossRef] [PubMed]

104. Guo, M.; Wei, L.; Yan, H.; Duan, Z.; Niu, Z.; Xiao, C. Exposure to ambient air pollution during trimesters of pregnancy and childhood allergic diseases in Wuhan, China. *Int. J. Environ. Health Res.* **2022**, *32*, 1962–1972. [CrossRef] [PubMed]

105. Luo, X.; Hong, H.; Lu, Y.; Deng, S.; Wu, N.; Zhou, Q.; Chen, Z.; Feng, P.; Zhou, Y.; Tao, J.; et al. Impact of air pollution and meteorological factors on incidence of allergic rhinitis: A low-latitude multi-city study in China. *Allergy* **2023**, *00*, 1–4. [CrossRef] [PubMed]

106. Andrade, C. Understanding relative risk, odds ratio, and related terms: As simple as it can get. *J. Clin. Psychiatry* **2015**, *76*, e857–e861. [CrossRef]

107. Slama, A.; Sliwczynski, A.; Woznica-Pyzikiewicz, J.; Zdrolik, M.; Wisnicki, B.; Kubajek, J.; Turzanska-Wieczorek, O.; Studnicki, M.; Wierzba, W.; Franek, E. The short-term effects of air pollution on respiratory disease hospitalizations in 5 cities in Poland: Comparison of time-series and case-crossover analyses. *Environ. Sci. Pollut. Res. Int.* **2020**, *27*, 24582–24590. [CrossRef]

108. Li, S.; Wang, G.; Wang, B.; Cao, S.; Zhang, K.; Duan, X.; Wu, W. Has the Risk of Outpatient Visits for Allergic Rhinitis, Related to Short-Term Exposure to Air Pollution, Changed over the Past Years in Beijing, China? *Int. J. Environ. Res. Public Health* **2022**, *19*, 12529. [CrossRef]

109. Liu, K.; Li, S.; Qian, Z.M.; Dharmage, S.C.; Bloom, M.S.; Heinrich, J.; Jalaludin, B.; Markevych, I.; Morawska, L.; Knibbs, L.D. Benefits of influenza vaccination on the associations between ambient air pollution and allergic respiratory diseases in children and adolescents: New insights from the Seven Northeastern Cities study in China. *Environ. Pollut.* **2020**, *256*, 113434. [CrossRef]

110. Zhou, P.E.; Qian, Z.; McMillin, S.E.; Vaughn, M.G.; Xie, Z.Y.; Xu, Y.J.; Lin, L.Z.; Hu, L.W.; Yang, B.Y.; Zeng, X.W. Relationships between long-term ozone exposure and allergic rhinitis and bronchitic symptoms in Chinese children. *Toxics* **2021**, *9*, 221. [CrossRef]

111. Miettine, O.S. Propotion of disease caused or prevented by a given exposure, trait or prevented by a given exposure. *Am. J. Epidemiol.* **1974**, *99*, 325–332. [CrossRef] [PubMed]

112. Gao, C.; Xiu, A.; Zhang, X.; Chen, W.; Liu, Y.; Zhao, H.; Zhang, S. Spatiotemporal characteristics of ozone pollution and policy implications in Northeast China. *Atmos. Pollut. Res.* **2020**, *11*, 357–369. [CrossRef]

113. Munir, S.; Chen, H.; Ropkins, K. Modelling the impact of road traffic on ground level ozone concentration using a quantile regression approach. *Atmos. Environ.* **2012**, *60*, 283–291. [CrossRef]

114. Vingarzan, R. A review of surface ozone background levels and trends. *Atmos. Environ.* **2004**, *38*, 3431–3442. [CrossRef]

115. Liu, Z.; Liu, S.; Hu, F.; Li, J.; Ma, Y.; Liu, H. A comparison study of the simulation accuracy between WRF and MM5 in simulating local atmospheric circulations over Greater Beijing. *Sci. China Earth Sci.* **2011**, *55*, 418–427. [CrossRef]

116. He, J.J.; Yu, Y.; Yu, L.J.; Liu, N.; Zhao, S.P. Impacts of uncertainty in land surface information on simulated surface temperature and precipitation over China. *Int. J. Climatol.* **2017**, *37*, 829–847. [CrossRef]

117. Kong, X.; Wang, A.; Bi, X.; Wang, D. Assessment of temperature extremes in China using RegCM4 and WRF. *Adv. Atmos. Sci.* **2019**, *36*, 363–377. [CrossRef]

118. Yan, D.; Liu, T.; Dong, W.; Liao, X.; Luo, S.; Wu, K.; Zhu, X.; Zheng, Z.; Wen, X. Integrating remote sensing data with WRF model for improved 2-m temperature and humidity simulations in China. *Dyn. Atmos. Oceans* **2020**, *89*, 101127. [CrossRef]

119. Liao, J.; Wang, T.; Wang, X.; Xie, M.; Jiang, Z.; Huang, X.; Zhu, J. Impacts of different urban canopy schemes in WRF/Chem on regional climate and air quality in Yangtze River Delta, China. *Atmos. Res.* **2014**, *145–146*, 226–243. [CrossRef]

120. Schicker, I.; Arias, D.A.; Seibert, P. Influences of updated land-use datasets on WRF simulations for two Austrian regions. *Meteorol. Atmos. Phys.* **2015**, *128*, 279–301. [CrossRef]

121. Tao, Z.; Chin, M.; Gao, M.; Kucsera, T.; Kim, D.; Bian, H.; Kurokawa, J.I.; Wang, Y.; Liu, Z.; Carmichael, G.R. Evaluation of NU-WRF model performance on air quality simulation under various model resolutions–an investigation within the framework of MICS-Asia Phase III. *Atmos. Chem. Phys.* **2020**, *20*, 2319–2339. [CrossRef]

122. Fuertes, E.; Standl, M.; Cyrys, J.; Berdel, D.; von Berg, A.; Bauer, C.P.; Kramer, U.; Sugiri, D.; Lehmann, I.; Koletzko, S.; et al. A longitudinal analysis of associations between traffic-related air pollution with asthma, allergies and sensitization in the GINIplus and LISAplus birth cohorts. *PeerJ* **2013**, *1*, 20. [CrossRef]

123. Gehring, U.; Wijga, A.H.; Hoek, G.; Bellander, T.; Berdel, D.; Bruske, I.; Fuertes, E.; Gruzieva, O.; Heinrich, J.; Hoffmann, B.; et al. Exposure to air pollution and development of asthma and rhinoconjunctivitis throughout childhood and adolescence: A population-based birth cohort study. *Lancet Respir. Med.* **2015**, *3*, 933–942. [CrossRef] [PubMed]

124. Pindus, M.; Orru, H.; Maasikmets, M.; Kaasik, M.; Jogi, R. Association Between Health Symptoms and Particulate Matter from Traffic and Residential Heating—Results from RHINE III in Tartu. *Open Respir. Med. J.* **2016**, *10*, 58–69. [CrossRef] [PubMed]

125. Burte, E.; Leynaert, B.; Marcon, A.; Bousquet, J.; Benmerad, M.; Bono, R.; Jacquemin, B. Long-term air pollution exposure is associated with increased severity of rhinitis in 2 European cohorts. *J. Allergy Clin. Immunol.* **2020**, *145*, 834–842. [CrossRef] [PubMed]

126. Burte, E.; Leynaert, B.; Bono, R.; Brunekreef, B.; Bousquet, J.; Carsin, A.E.; Jacquemin, B. Association between air pollution and rhinitis incidence in two European cohorts. *Environ. Int.* **2018**, *115*, 257–266. [CrossRef]

127. Liu, H.Y.; Skjetne, E.; Kobernus, M. Mobile phone tracking: In support of modelling traffic-related air pollution contribution to individual exposure and its implications for public health impact assessment. *Environ. Health* **2013**, *12*, 1–12. [CrossRef]

128. Steinle, S.; Reis, S.; Sabel, C.E.; Semple, S.; Twigg, M.M.; Braban, C.F.; Leeson, S.R.; Heal, M.R.; Harrison, D.; Lin, C.; et al. Personal exposure monitoring of PM$_{2.5}$ in indoor and outdoor microenvironments. *Sci. Total Environ.* **2015**, *508*, 383–394. [CrossRef]

129. Park, Y.M. Assessing personal exposure to traffic-related air pollution using individual travel-activity diary data and an on-road source air dispersion model. *Health Place* **2020**, *63*, 102351. [CrossRef]

130. Haga, S.L.; Hagenbjörk, A.; Olin, A.C.; Forsberg, B.; Liljelind, I.; Carlsen, H.K.; Modig, L. Personal exposure levels to O_3, NO_x and PM_{10} and the association to ambient levels in two Swedish cities. *Environ. Monit. Assess.* **2021**, *193*, 674. [CrossRef]

131. Taştan, M.; Gökozan, H.J. Real-time monitoring of indoor air quality with internet of things-based E-nose. *Appl. Sci.* **2019**, *9*, 3435. [CrossRef]

132. Chatzidiakou, L.; Krause, A.; Popoola, O.A.M.; Di Antonio, A.; Kellaway, M.; Han, Y.; Squires, F.A.; Wang, T.; Zhang, H.; Wang, Q.; et al. Characterising low-cost sensors in highly portable platforms to quantify personal exposure in diverse environments. *Atmos. Meas. Tech.* **2019**, *12*, 4643–4657. [CrossRef] [PubMed]

133. Liu, M.; Barkjohn, K.K.; Norris, C.; Schauer, J.J.; Zhang, J.; Zhang, Y.; Hu, M.; Bergin, M. Using low-cost sensors to monitor indoor, outdoor, and personal ozone concentrations in Beijing, China. *Environ. Sci. Process. Impacts* **2020**, *22*, 131–143. [CrossRef] [PubMed]

134. Park, Y.M.; Kwan, M.P. Individual exposure estimates may be erroneous when spatiotemporal variability of air pollution and human mobility are ignored. *Health Place* **2017**, *43*, 85–94. [CrossRef]

135. Lee, D.H.; Kim, S.H.; Kang, S.H.; Kwon, O.K.; Park, J.J.; Yoon, C.H.; Cho, Y.S.; Heo, J.; Yi, S.M.; Youn, T.J.; et al. Personal exposure to fine particulate air pollutants impacts blood pressure and heart rate variability. *Sci. Rep.* **2020**, *10*, 16538. [CrossRef] [PubMed]

136. Cao, R.; Wang, Y.; Huang, J.; Zeng, Q.; Pan, X.; Li, G.; He, T. The construction of the air quality health index (AQHI) and a validity comparison based on three different methods. *Environ. Res.* **2021**, *197*, 110987. [CrossRef] [PubMed]

137. Li, L.; Lin, G.Z.; Liu, H.Z.; Guo, Y.M.; Ou, C.Q.; Chen, P.Y. Can the Air Pollution Index be used to communicate the health risks of air pollution? *Environ. Pollut.* **2015**, *205*, 153–160. [CrossRef] [PubMed]

138. Zhang, Q.; Chen, R.; Yin, G.; Du, X.; Meng, X.; Qiu, Y.; Zhou, M. The establishment of a new air health index integrating the mortality risks due to ambient air pollution and non-optimum temperature. *Engineering* **2022**, *14*, 156–162. [CrossRef]

139. Wong, T.W.; Tam, W.W.S.; Yu, I.T.S.; Lau, A.K.H.; Pang, S.W.; Wong, A.H.S. Developing a risk-based air quality health index. *Atmos. Environ.* **2013**, *76*, 52–58. [CrossRef]

140. Szyszkowicz, M. The Air Quality Health Index and all emergency department visits. *Environ. Sci. Pollut. Res.* **2019**, *26*, 24357–24361. [CrossRef]

141. Olstrup, H.; Johansson, C.; Forsberg, B.; Tornevi, A.; Ekebom, A.; Meister, K. A multi-pollutant air quality health index (AQHI) based on short-term respiratory effects in Stockholm, Sweden. *Int. J. Environ. Res. Public Health* **2019**, *16*, 105. [CrossRef]

142. Gladson, L.A.; Cromar, K.R.; Ghazipura, M.; Knowland, K.E.; Keller, C.A.; Duncan, B. Communicating respiratory health risk among children using a global air quality index. *Environ. Int.* **2022**, *159*, 107023. [CrossRef] [PubMed]